UPPSALA
UNIVERSITET

Digital Comprehensive Summaries of Uppsala Dissertations from the Faculty of Science and Technology 1542

Analysis and control of magnetic forces in synchronous machines

J. J. PÉREZ-LOYA

ACTA
UNIVERSITATIS
UPSALIENSIS
UPPSALA
2017

ISSN 1651-6214
ISBN 978-91-513-0036-8
urn:nbn:se:uu:diva-328086

Dissertation presented at Uppsala University to be publicly examined in Häggsalen, Ångströmlaboratoriet, Lägerhyddsvägen 1, Uppsala, Friday, 6 October 2017 at 13:15 for the degree of Doctor of Philosophy. The examination will be conducted in English. Faculty examiner: Professor Anouar Belahcen (Aalto University).

Abstract
Pérez-Loya, J. J. 2017. Analysis and control of magnetic forces in synchronous machines. *Digital Comprehensive Summaries of Uppsala Dissertations from the Faculty of Science and Technology* 1542. 84 pp. Uppsala: Acta Universitatis Upsaliensis. ISBN 978-91-513-0036-8.

In a synchronous machine, radial, tangential, and axial forces are generated. In this thesis, three different technologies to control them are proposed. The first one, involves the utilization of the radial forces that arise between the rotor and the stator. This is achieved by segmenting the rotor field winding into groups of poles and controlling their corresponding magnetization individually. This technology is particularly useful to achieve magnetic balance and to create controllable radial forces. The second technology, involves the control of the rotor field in order to influence the tangential forces that produce torque. This is achieved by inverting the rotor field winding polarity with respect to the stator field. With this technique, breaking and accelerating torques can be created. It is particularly useful to start a synchronous machine. Finally, the application of axial forces with a magnetic thrust bearing is discussed. The main benefits of this technology are higher efficiency and increased reliability.

The work presented in this thesis was carried out within the Division of Electricity in the Department of Engineering Sciences at Uppsala University. It is based on original research supported by analytical calculations, computational simulations and extensive experimental work.

Keywords: eccentricity, electromagnetics, electromagnetic forces, excitation, magnetic fields, magnetic forces, magnetic thrust bearing, rotor drive, split rotor, starting, synchronous generators, synchronous machines, synchronous motors, unbalanced magnetic pull

J. J. Pérez-Loya, Department of Engineering Sciences, Electricity, Box 534, Uppsala University, SE-75121 Uppsala, Sweden.

ISSN 1651-6214
ISBN 978-91-513-0036-8
urn:nbn:se:uu:diva-328086 (http://urn.kb.se/resolve?urn=urn:nbn:se:uu:diva-328086)

Dedicada a mi familia.
Pasada, presente y futura.

List of papers

This thesis is based on the following papers, which are referred to in the text by their Roman numerals.

I **Pérez-Loya, J. J.**, Lundin, U. (2014) "Optimization of force between cylindrical permanent magnets". *IEEE Magnetics Letters, vol. 5, pp. 1-4, October 2014.*

II **Pérez-Loya, J. J.**, Lundin, U. (2016) "Simple method to calculate the force between thin walled solenoids". *Progress in Electromagnetics Research M, vol. 51, pp. 93-100, October 2016.*

III **Pérez-Loya, J. J.**, Abrahamsson, C. J. D., Lundin, U. (2017) "Demonstration of active compensation of unbalanced magnetic pull in synchronous machines". *CIGRE Science & Engineering, vol. 8, pp. 98-107, June 2017.*

IV **Pérez-Loya, J. J.**, Abrahamsson, C. J. D., Lundin, U. (2017) "Electromagnetic losses in synchronous machines during active compensation of unbalanced magnetic pull due to static eccentricity". *Accepted for publication in IEEE Transactions on Industrial Electronics.*

V **Pérez-Loya, J. J.**, Abrahamsson, C. J. D., Lundin, U. (2016) "Arrangement and method for force compensation in electrical machines, SE538502C2". *Swedish Patent and Registration Office.*

VI **Pérez-Loya, J. J.**, Abrahamsson, C. J. D., Evestedt, F. ,Lundin, U. (2017) "Demonstration of synchronous motor start by rotor polarity inversion". *Accepted with revisions in IEEE Transactions on Industrial Electronics.*

VII **Pérez-Loya, J. J.**, Abrahamsson, C. J. D., Lundin, U. (2017) "Synchronous machine and method for operating a synchronous machine, SE1750223-8". *Swedish Patent and Registration Office.*

VIII **Pérez-Loya, J. J.**, de Santiago, J., Lundin, U. (2013) "Construction of a permanent magnet thrust bearing for a hydropower generator test setup". *Proceedings of the 1st Brazilian Workshop on Magnetic Bearings.*

IX **Pérez-Loya, J. J.**, Rodriguez, E., Hedlund, M., Stephan, R. M., Lundin, U. (2013) "Magnetic modeling and measurement of forces between permanent magnet rings used as passive magnetic bearings". *Proceedings of the 1st Brazilian Workshop on Magnetic Bearings.*

X **Pérez-Loya, J. J.**, Abrahamsson, C. J. D., Evestedt, F., Lundin, U. (2016) "Initial performance tests of a permanent magnet thrust bearing for a hydropower synchronous generator test-rig". *Proceedings of Advances in Magnetics, 2016.*

XI **Pérez-Loya, J. J.**, Abrahamsson, C. J. D., Evestedt, F., Lundin, U. (2017) "Performance tests of a permanent magnet thrust bearing for a hydropower synchronous generator test-rig". *Accepted for publication in ACES Journal.*

XII Abrahamsson, C. J. D., **Pérez-Loya, J. J.**, Evestedt, F., Lundin, U. (2017) "Magnetic thrust bearing for a hydropower unit with a Kaplan turbine". *Unpublished manuscript.*

XIII **Pérez-Loya, J. J.**, Abrahamsson, C. J. D., Lundin, U. (2016) "Arrangement for supporting a rotatable body, EP16196073". *European Patent Office.*

XIV **Pérez-Loya, J. J.**, Abrahamsson, C. J. D., Lundin, U. (2016) "Fail-safe system for discharging a magnetic thrust bearing, EP16200156". *European Patent Office.*

XV Hedlund, M., Abrahamsson, J., **Pérez-Loya, J. J.**, Lundin, J., Bernhoff, H. (2013) "Passive axial thrust bearing for a flywheel energy storage system". *Proceedings of the 1st Brazilian Workshop on Magnetic Bearings.*

XVI Hedlund, M., Abrahamsson, C. J. D., **Pérez-Loya, J. J.**, Lundin, J., Bernhoff, H. (2017) "Eddy currents in a passive magnetic axial thrust bearing for a flywheel energy storage system". *International Journal of Applied Electromagnetics and Mechanics, vol. 54, no. 3, pp. 389-404, July 2017.*

XVII Rodriguez, E., de Santiago, J., **Pérez-Loya, J. J.**, Costa, F., Sotelo, G., Oliveira, J., Stephan, R. M. (2014) "Analysis of passive magnetic bearings for kinetic energy storage systems", *Proceedings of the 14th International Symposium on Magnetic Bearings.*

XVIII Rodriguez, E., **Pérez-Loya, J. J.**, de Santiago, J., Costa, F., Sotelo, G., Oliveira, J., Stephan, R.M. (2014) "Passive magnetic bearing system", *Proceedings of the 22nd International Conference on Magnetically Levitated Systems and Linear Drives.*

XIX Nøland, J., Evestedt, F., **Pérez-Loya, J. J.**, Abrahamsson, C. J. D., Lundin, U. (2016) "Design and characterization of a rotating brushless PM exciter for a synchronous generator test setup". *Proceedings of the XXII International Conference of Electric Machines.*

XX Nøland, J., Evestedt, F., **Pérez-Loya, J. J.**, Abrahamsson, C. J. D., Lundin, U. (2016) "Evaluation of different power electronic interfaces for control of a rotating brushless PM exciter". *Proceedings of the 42nd annual Conference of the IEEE Industrial Electronics Society.*

XXI Nøland, J., Evestedt, F., **Pérez-Loya, J. J.**, Abrahamsson, C. J. D., Lundin, U. (2017) "Design and characterization of a rotating brushless outer pole PM exciter for a synchronous generator". *IEEE Transactions on Industry Applications, vol. 53, no. 3, pp. 2016-2027, May 2017.*

XXII Nøland, J., Evestedt, F., **Pérez-Loya, J. J.**, Abrahamsson, C. J. D., Lundin, U. (2017) "Testing of active rectification topologies on a six-phase rotating brushless outer pole PM exciter". *Accepted with revisions in IEEE Transactions on Energy Conversion.*

XXIII Nøland, J., Evestedt, F., **Pérez-Loya, J. J.**, Abrahamsson, C. J. D., Lundin, U. (2017) "Comparison of thyristor rectifier configurations for a six-phase rotating brushless outer pole PM exciter". *Accepted for publication in IEEE transactions on Industrial Electronics.*

Reprints were made with permission from the publishers.

Contents

1. Introduction

The synchronous machine has been constantly improved since its invention in 1887 when Friedrich August Haselwander introduced the salient pole type. A few years later, in 1898 and 1901, Charles E. Brown introduced, respectively, laminated and solid cylindrical rotors. These topologies are still used today. Synchronous machines are remarkably efficient. The 210 kW generator of the Lauffen am Neckar hydropower plant, which in 1891 delivered power to the Frankfurt exposition 175 km away, had an efficiency of 96.5% [1]. A 10 MW synchronous machine commissioned in 1998 at the Porjus hydropower plant in the north of Sweden, generator Porjus U9, has an efficiency, from shaft to grid at rated load, of 98%. Recently, ABB announced a new world record in efficiency for synchronous motors reaching 99.05% in laboratory tests performed on a 44 MW machine.

Besides being efficient, synchronous machines are reliable, they are expected to last for decades, are utilized in harsh environments, and have the possibility to produce or consume reactive power. It is by far the most utilized machine in the power generation industry.

Some of the main drawbacks of the synchronous machine are that it requires an excitation system, it has a relatively high initial cost, and does not have self starting capabilities. Those are some of the reasons why, when it comes to motors, it is utilized only in special applications.

During the operation of a synchronous machine, either as a motor or generator, radial, tangential, and axial forces are generated. In order to further improve the performance of these machines, in this work, the use of three technologies related to these forces is proposed. The first one, involves the control of the radial forces that arise between the rotor and the stator of a synchronous machine, it is particularly useful to achieve magnetic balance. The second one, involves the control of the rotor field in order to influence the tangential forces, it is particularly useful to start a machine. Finally, the application of axial forces with an external actuator, a magnetic thrust bearing, is discussed.

1.1 Magnetic forces in synchronous machines

In practice, there are two ways to create magnetic forces that are useful in the context of this thesis, either with electromagnets or permanent magnets. Permanent magnets are created by aligning the ferromagnetic domains of a hard magnetic material. Once this is done the material becomes permanently magnetized, hence the name. The magnet will remain in that state if properly utilized. There is no need to apply an external field to keep them magnetized.

In order to produce a magnetic field from an electromagnet, a sustained electrical current is necessary. An electromagnet is basically a conductor wound around a core. The core should be manufactured from a soft magnetic steel, as it has a B-H curve that is relatively narrow in the axis of the abscissas and relatively high in the axis of the ordinates. The notion of soft, means that it is easy to magnetize and demagnetize. The implication is that the magnetic domains within the material are easily aligned in the direction of an applied magnetizing field, resulting in a large magnetic flux density. When the magnetizing field is removed, most of the domains become misaligned. Some of them though, stay aligned producing a remanent field, like in a permanent magnet but very small in comparison. Since electromagnets are soft, it is not possible to use them to create repulsive forces, that is an advantage of permanent magnets. When two similar electromagnets subjected to fields with similar intensities but opposite polarities are faced against each other, the force will result from the superposition of both fields applied in both cores. Most of the magnetic domains will be aligned in the direction of the resulting field, thus yielding a very small attractive force or no force at all. That is why, electromagnets are only utilized to create attractive forces. Even though, a sustained current is needed to magnetize them, electromagnets can be controlled. This is a considerable advantage when compared to permanent magnets.

The rotor poles of a synchronous machine can be controlled in order to influence the resulting radial and tangential forces between the rotor and the stator. When it comes to axial forces, additional actuators are needed.

Radial forces

The synchronous machine is efficient and reliable, but it is not without challenges. For instance, unbalanced magnetic pull is a problem that has persisted for over a century [2–5]. It is caused by imperfections in the magnetic field crossing the air gap of electrical machines. It creates noise, losses, rotor dynamic problems, increased wear, and tear that leads to decreased availability and shorter machine lifetimes. It can be severe, particularly in large machines like hydropower generators. Therefore, it is important to protect the machines from its negative effects [6]. In Sweden, extensive research has been conducted in the topic for more than a decade [7–12]. Unbalanced magnetic pull has also been reported in other applications [13, 14], and for other types of

machines, particularly induction machines [15–17]. Magnetic forces, mainly in induction machines, have been thoroughly investigated in Finland for more than 15 years [18–25].

Unbalanced magnetic pull can be diagnosed, for example, by force measurements [26], by utilizing search coils [27, 28], measurement of the magnetic flux density with Hall sensors [29], from noise measurements [30], from currents and vibration measurements [31], from harmonic signatures in the stator voltages [32], and from the analysis of split phase currents [33, 34], just to name a few methods.

The traditional solutions utilized to address the negative effects of unbalanced magnetic pull are the utilization of damper windings [35–37], and the use of parallel circuits [38–40]. The addition of actively controlled compensating windings in the stator of induction machines has also been proposed [41, 42].

In this thesis, a technique that allows the creation radial magnetic forces between the rotor and stator of the machines is presented. These forces can be utilized, for example, to achieve magnetic balance in order to eliminate unbalanced magnetic pull.

Tangential forces

Another challenge associated with synchronous machines is that they do not have self start capabilities. It is relatively difficult to start them, particularly large motors [43]. To be able to produce a starting torque, a frequency converter can be utilized. Another technique is asynchronous start [44], in this case, a damper cage or a solid rotor is needed. For small motors, direct on line is the most common method of asynchronous start. For large machines, auxiliary motors can be utilized [45].

The lack of self starting capability is an undesirable characteristic that the synchronous motor shares with permanent magnet synchronous motors and synchronous reluctance motors. The fact that these types of motors are not self starting and require a frequency converter has hindered their acceptance in applications that do not require variable speed.

In a similar way as for the synchronous motors, damper cages are utilized in permanent magnet synchronous motors and in synchronous reluctance motors to be able to achieve an asynchronous start [46–51]. Adding a damper cage increases the initial cost of the machine and favors the utilization of other types of motors instead.

In this thesis, a technique to control the tangential forces within the machine in order influence the produced torque is presented. This technique is particularly useful during the start of a motor.

Axial forces

As opposed to radial and tangential forces, a significant amount of axial magnetic forces can not be created by the synchronous machine itself. Additional magnets, in the form of magnetic thrust bearings are required.

In today's context, magnetic thrust bearings are relatively common in high speed machines, normally horizontal axis. Their purpose is, together with radial magnetic bearings, to levitate the machine.

However, vertical axis synchronous machines are most likely the oldest application of magnetic thrust bearings. They have been in use since the 1950's, they were developed and introduced to the market by Fuji Denki.

The idea behind these magnetic thrust bearings is to act as a thrust compensator for a mechanical thrust bearing. The main purpose was to reduce the overall losses in the thrust bearing system. This is achieved by reducing the thrust load on the mechanical bearing. Additionally, its size can be reduced which increases further the performance since the losses in a mechanical thrust bearing are heavily dependant on its dimensions [52, 53].

The first magnetic thrust bearing installation reported by Fuji was in a synchronous condenser [54]. But it is know that before that, in Soviet Russia, a magnetic thrust bearing was utilized to reduce the load on the mechanical thrust bearing of a super sized low speed Kaplan turbine which, without magnetic support, was not possible to realize at that time [55]. Over the years, magnetic thrust bearings for hydropower have been also utilized in Pelton turbines [56], in pump storage stations, to reduce the torque during start operations [57, 58], to test thrust bearings [59], even small stations have been fully levitated [60].

By 1964, Fuji Denki had supplied eight machines with magnetic thrust bearings with capacities from 33 to 288 ton with outputs between 13 MVA and 70 MVA [61]. In 1980, test site reports of a large capacity pump storage station with two generator/motor units of 220 MVA equipped with magnetic thrust bearings with a capacity of nearly 400 ton are published [62]. They were followed by two more pump storage stations with two units each with ratings of 385 MVA and 250 MVA, respectively [63].

The first magnetic thrust bearing installation in Europe is in the Dinorwig Power station in the United Kingdom. It is one of the largest pump storage stations in the world. After nearly twenty years of operation with numerous thrust bearing failures, one of the units was upgraded by Voith Fuji with a magnetic thrust bearing. At the time of modernization, the station had the fastest time response in Europe. It's operation was particularly severe for the thrust bearing with a pressure of 5 MPa at 500 rpm and around 20 to 25 changes in the direction of rotation per day. After the upgrade, the bearing pad temperature and pressure were reduced by 20°C and by forty percent, respectively [64, 65].

In this thesis, a permanent magnet thrust bearing for a vertical synchronous machine test rig and a magnetic thrust bearing designed to take the full load in a hydropower generator with a Kaplan turbine are presented.

1.2 Thesis structure

This thesis is a brief summary of the main work I have done during my time as a PhD candidate at Uppsala University. This endeavor was only possible due to the competence that my colleagues at the University have accumulated during many years and hopefully this thesis contributes to my colleagues to come. During these years of work with applied magnetics, there has been a recurring question in my mind:

How can we use magnetic forces to improve the performance of synchronous machines?

This question is addressed in this thesis which is divided into three parts. In the first one, relevant theoretical background is briefly introduced. In the second part, the experimental equipment and the experiments utilized in the preparation of some of the papers in which this thesis is based are described. Finally, in the third part, the findings are presented.

Part I:
Theoretical Background

2. Magnetic forces

2.1 Analytical force calculation between permanent magnets

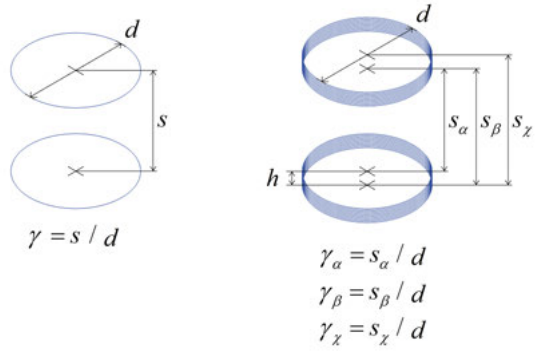

Figure 2.1. (Left) Schematic of two infinitesimally thin concentric rings. (Right) Schematic of two identical concentric thin walled solenoids. Reproduced courtesy of The Electromagnetics Academy

The force between two ideal permanent magnets can be calculated in the same way as the force between two thin walled solenoids. With that notion in mind, the following equations are derived from the formulations presented by Garret [66] and Iwasa [67], which in turn are derived from Maxwell [68]. For a system with a pair of identical coaxial cylindrical magnets, the force can be calculated from:

$$\begin{aligned} F_{sz} = \frac{B_r^2 A}{2\mu_0} \Bigg\{ & \sqrt{1+(\alpha+\gamma_\alpha)^2}(8/\pi)(\alpha+\gamma_\alpha)[K(k_1)-E(k_1)] \\ & -\sqrt{1+(2\alpha+\gamma_\alpha)^2}(4/\pi)(2\alpha+\gamma_\alpha)[K(k_2)-E(k_2)] \\ & -\sqrt{1+\gamma_\alpha^2}(4/\pi)(\gamma_\alpha)[K(k_3)-E(k_3)] \Bigg\}. \end{aligned} \tag{2.1}$$

Where B_r is the remanent field of the permanent magnets, A their facing cross sectional area, α the height to diameter ratio of each magnet, and γ_α is the ratio of the separation between the magnets and their diameter, as shown in

fig. 2.1(Right). $K(k)$ and $E(k)$ are the complete elliptic integrals of the first and second kind. The moduli k_1, k_2, and k_3 are:

$$k_1^2 = \frac{1}{1+(\alpha+\gamma_\alpha)^2}, \tag{2.2}$$

$$k_2^2 = \frac{1}{1+(2\alpha+\gamma_\alpha)^2}, \tag{2.3}$$

$$k_3^2 = \frac{1}{1+\gamma_\alpha^2}. \tag{2.4}$$

With eqs. (2.1) to (2.4), it is possible to calculate magnetic forces between identical cylindrical permanent magnets utilizing complete elliptic integrals of the first and second kind.

2.2 Simplification of analytical force calculations between permanent magnets

To simplify the calculation of the forces between two thin walled solenoids and by consequence between two permanent magnets, the use of elliptical integrals can be circumvented. Please consider the force between two infinitesimally thin concentric rings as shown in fig. 2.1(Left). The force between them, can be expressed as:

$$F_{ab} = \frac{\mu_0}{2} i_a i_b f''(\gamma). \tag{2.5}$$

Where i_a and i_b are the electrical currents circulating in each of them, s is the separation between the rings, d their diameter, and $f''(\gamma)$ is a function that accounts for the geometry of the rings according to $\gamma = s/d$. The integration of the force between thin concentric rings yields the force between thin walled solenoids. One way to achieve it, is by writing the expression in the form of the Riemman integral a couple of times. After doing so, the following expression for the force between two identical concentric thin walled solenoids is achieved:

$$F_{sz} = \frac{\mu_0}{2} \frac{I_s I_z}{(\gamma_\beta - \gamma_\alpha)^2} [f(\gamma_\chi) - 2f(\gamma_\beta) + f(\gamma_\alpha)]. \tag{2.6}$$

Where, I_s and I_z are the surface currents in each solenoid, γ_α, γ_β, and γ_χ are the separation to diameter ratios, and $f(\gamma_\alpha)$, $f(\gamma_\beta)$, $f(\gamma_\chi)$ are evaluations of a function $f(\gamma)$ that can be found from a carefully designed experiment, from finite element simulations, or from existing solutions. One possible expression for it is the following:

$$f(\gamma) = \frac{A\gamma^4 + B\gamma^3 + C\gamma^2 + D\gamma + E}{\gamma + F}. \tag{2.7}$$

Table 2.1. *Coefficients for eq.* (2.7)

A=0.001032	B=-0.014560	C=4.069000
D=0.209100	E=-0.005901	F=0.294100

Equation (2.7) and the coefficients shown in table 2.1 are obtained from a curve fit of the double numerical integration of $f''(\gamma)$, and validated for for height to diameter ratios $0.2 \leq \alpha \leq 2$, and separation to diameter ratios from $\gamma_\alpha = 0.01$ until the ratio is so large that the force between the magnets is only 5% of the maximum force. $f''(\gamma)$ is obtained from the following semi analytical solution:

$$f''(\gamma) = \sqrt{\frac{1}{\gamma^2}+1}\left\{k^2K(k)+(k^2-2)[K(k)-E(k)]\right\}, \tag{2.8}$$

the modulus k is:

$$k^2 = \frac{1}{1+\gamma^2}. \tag{2.9}$$

2.3 Real and ideal permanent magnets

There are several techniques available to model ideal permanent magnets. Notably, they can be represented with the Coulomb approach [69] as magnetic charges, or they can be modelled as thin walled solenoids [66–68]. In the work presented in this thesis, the later, which is sometimes also referred as the Ampére model, is utilized.

In simple terms, in an ideal permanent magnet, all the ferromagnetic domains available within the material are hardly magnetized. The implication is that for a given magnet with remanence B_r its corresponding ideal coercivity H_{cmax}, which is the maximum that can be theoretically achieved for that remanence, is defined according to:

$$H_{cmax} = -B_r/\mu_0. \tag{2.10}$$

Where μ_0 is the permeability of free space. In an ideal permanent magnet, the aligned magnetic domains contribute exactly as an electrical current that flows in an infinitesimally thin surface perpendicular to the direction of the magnet's own magnetization would contribute. The B-H curve of such an ideal permanent magnet is a straight line in which the interception in the axis of the ordinates is the magnet remanence B_r and the interception in the axis of the abscissas is the ideal magnet coercivity H_{cmax}. In real permanent magnets, this is never the case. The coercivity of the magnets never reaches the ideal point. Typical B-H curves for different permanent magnet materials and their

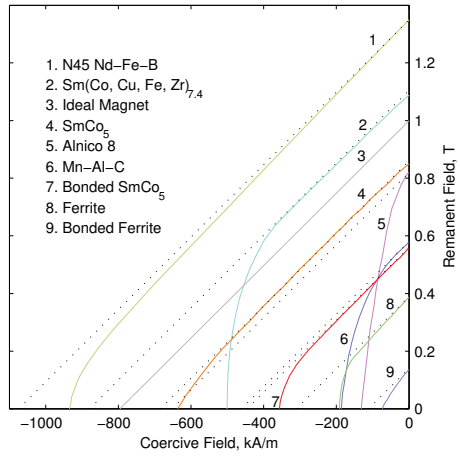

Figure 2.2. B-H curves for different permanent magnet materials. Copyright © 2014, IEEE

corresponding ideal B-H curve (dotted lines) are shown in fig. 2.2. Note that for the Ideal Magnet, the solid and dotted line overlap.

By comparing the typical and ideal B-H curves, it can be concluded that in a permanent magnet it is desirable to have a high remanent field, but also a high coercivity. To some extent, the degree of remanence and coercivity of a magnet indicates how many magnetic domains are aligned in the same direction and how stiff they are.

In analytical force calculations, permanent magnets are assumed to be ideal. The output of the calculations is usually an overestimation. Acceptable if the B-H curve of the real permanent magnet do not deviate considerably from its ideal counterpart.

In all B-H curves, irrespective of the permanent magnet material utilized, the deviation between real and ideal curves is smaller in the region closer to the ordinate axis. As the demagnetizing field, H, increases, the deviation between the ideal and non ideal permanent magnets increases.

The point of operation of the individual magnetic domains in the permanent magnet is determined by the geometry of the magnet and the presence of external fields. The height to diameter ratio of the magnets defines in which point along the B-H curve the magnetic domains operate when they are not subjected to any external influence. The domains on relatively thick magnets operate closer to the ordinate axis, while on shallow magnets operate further in the direction of -H. If external fields are applied they will have an influence on these points. Magnetizing fields, those that are in the direction of magnetization of the magnet, will push the operating points of the individual domains in the direction of +H. While demagnetizing fields, those that are 180° from the direction of magnetization will push them in the direction of -H.

When a permanent magnet can not be considered ideal, high accuracy is required, or complex geometries are used, it is advisable to use the finite element method rather than analytical models to calculate magnetic forces.

2.4 Analytical force calculation in electromagnets

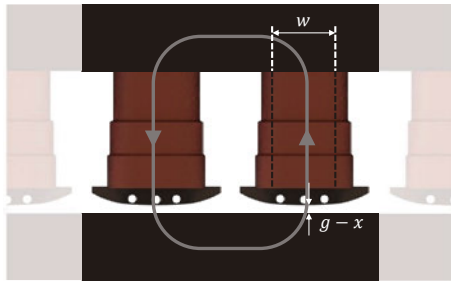

Figure 2.3. Section of a hypothetical electromagnet.

Please consider a segment of an electromagnet as shown in fig. 2.3, in which an electrical current I flows through N number of turns of conductive wire wound around a laminated core of high permeability steel with cross sectional area $A = wh$, where w and h are, respectively, the width and height of the cross section. The air gap surface area is $S = 2A$. Within the core, the magnetic flux ϕ (indicated by the gray line) associated with the electrical current I is enhanced. The flux crosses the air gap which has a total length $l = 2(g-x)$, where g is the nominal air gap length, and x is a length deviation. Since, disregarding the effects of magnetic saturation, the relative permeability of steel ($1000 \leq \mu_{rs} \leq 10000$) is a few orders of magnitude higher than the relative permeability of air ($\mu_a = 1$), its reluctance can be neglected. The core is laminated, therefore the effect of eddy currents can also be ignored. The reluctance of the electromagnet becomes:

$$R = \frac{l}{\mu_0 A} = \frac{2(g-x)}{\mu_0 A}. \tag{2.11}$$

Where μ_0 is the permeability of free space. The inductance of such a magnetic circuit is:

$$L = \frac{N^2}{R}. \tag{2.12}$$

Therefore, by combining eq. (2.11) and eq. (2.12), the inductance of the electromagnet can be expressed as:

$$L = \left(\frac{N^2 \mu_0 A}{2g}\right)\left(\frac{1}{1-\frac{x}{g}}\right). \tag{2.13}$$

If the first term is defined as the nominal inductance, L_n, and the second term is replaced by the first two terms of a Maclaurin series, eq. (2.13) becomes:

$$L = (L_n)\left(1 + \frac{x}{g}\right). \tag{2.14}$$

In a linear system, like the one described, the magnetic energy of an electromagnet is:

$$W = \frac{1}{2}LI^2, \tag{2.15}$$

and the magnetic force:

$$F = \frac{\partial W}{\partial x}. \tag{2.16}$$

Combining eq. (2.15) and eq. (2.16) yields:

$$F = \frac{\partial L}{\partial x}\frac{I^2}{2}. \tag{2.17}$$

By inserting eq. (2.14) in eq. (2.17), the relationship between the electrical current in the coil and the force in the electromagnet becomes:

$$F = \frac{L_n}{g}\frac{I^2}{2}. \tag{2.18}$$

In general, the magnetic flux density is defined as:

$$B = \frac{\phi}{A}. \tag{2.19}$$

In a magnetic circuit, the relationship between the current in a coil and the magnetic flux density B becomes:

$$NI = \phi R = \frac{Bl}{\mu_0}. \tag{2.20}$$

For the magnetic circuit described, when $x = 0$, the magnetic flux density is:

$$B = \frac{NI\mu_0}{l} = \frac{NI\mu_0}{2g}. \tag{2.21}$$

By combining eq. (2.13), eq. (2.18) and eq. (2.21), we find that the relationship between the magnetic force and the magnetic flux density is:

$$F = \frac{B^2 S}{2\mu_0}, \tag{2.22}$$

and the magnetic pressure can be defined as:

$$\sigma = \frac{B^2}{2\mu_0}. \tag{2.23}$$

2.5 Current and force control in an electromagnet

From a circuit theory point of view, the electromagnet described in section 2.4 is a resistor in series with an inductance. Since it is laminated, the effect of Eddy currents can be disregarded at relatively low frequencies. If the resistance is neglected, the relationship between V, the voltage applied across the terminals of the electromagnet and I, the resulting current can be expressed as:

$$V = L\frac{dI}{dt}. \tag{2.24}$$

By controlling the polarity of the applied voltage, a desired current in the electromagnet can be achieved. If positive voltage is applied, the current in the electromagnet will increase according to eq. (2.24), the opposite if a negative voltage is applied. In practice this can be done by utilizing a single phase inverter, also known as H bridge. A schematic drawing of such a circuit is shown in fig. 2.4. Having the possibility to control the current of an electromagnet is important. According to eq. (2.18), the magnetic force from an electromagnet depends on its current. By controlling the current in the electromagnet the force can also be controlled.

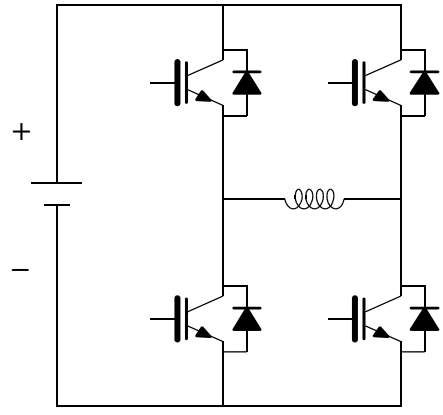

Figure 2.4. Inductor connected across an H bridge.

2.6 Current dynamics in an electromagnet

Please consider the following current waveform applied to the electromagnet described in section 2.4 with an H bridge as shown in fig. 2.4:

$$I = I_m + I_\Delta \sin(2\pi f t), \tag{2.25}$$

where I_m is a direct current component, I_Δ, f, and t are, respectively, the amplitude, the frequency of the sinusoidal component, and time. The maximum

slope for that waveform is:

$$\frac{dI}{dt}_{max} = I_{\Delta} 2\pi f. \tag{2.26}$$

From eq. (2.24), it can be seen that:

$$\frac{V}{L} = \frac{dI}{dt}. \tag{2.27}$$

Therefore, by combining eqs. (2.26) and (2.27), it can be concluded that in order to achieve the current dynamics required by the waveform described in eq. (2.25), the following relation has to be fulfilled:

$$\frac{V}{L} \geq I_{\Delta} 2\pi f. \tag{2.28}$$

2.7 Finite element formulation for force calculations

Magnets can be modelled with different levels of detail. For example, permanent magnets can be considered ideal, which yields the same result as the analytical calculations. They can be modelled taking into account eddy currents [70] or irreversible demagnetization [71]. When the effect of eddy currents can be neglected, and irreversible demagnetization is not a risk, they can be modelled taking only into account their magnetization characteristics. This can be done through the relative permeability. In that case, in the finite element formulation, the following constitutive relation can be used:

$$\mathbf{B} = \mu_0 \bar{\mu}_r \mathbf{H}. \tag{2.29}$$

Where the relative permeability for the permanent magnets is:

$$\bar{\mu}_r = \begin{bmatrix} 1 & 0 & 0 \\ 0 & 1 & 0 \\ 0 & 0 & \frac{B_z}{\mu_0 H_z} \end{bmatrix}, \tag{2.30}$$

for the surrounding air:

$$\bar{\mu}_r = 1. \tag{2.31}$$

The relationship between the magnetic flux density and the magnetic field $H_z = f(B_z)$, where z is the direction of magnetization, is obtained from the magnetization data of the permanent magnet materials. If only permanent magnets are involved in the calculation, the following equation is solved with the finite element method to find the field solution:

$$\nabla \times (\mu_0^{-1} \bar{\mu}_r^{-1} \nabla \times \mathbf{A}) = 0, \tag{2.32}$$

where:

$$\mathbf{B} = \nabla \times \mathbf{A}. \tag{2.33}$$

In a similar way as described for the permanent magnets, when electromagnets are modelled, the magnetic properties of steel, isotropic or anisotropic, can be introduced through the relative permeability tensor. However, since in electromagnets currents **J** are involved, eq. (2.32) becomes:

$$\nabla \times (\mu_0^{-1} \bar{\mu}_r^{-1} \nabla \times \mathbf{A}) = \mathbf{J}. \tag{2.34}$$

With the field solution at hand, magnetic forces can be calculated, for example, with the Maxwell stress tensor:

$$\sigma_{ij} = \frac{1}{\mu_0} B_i B_j - \frac{1}{2\mu_0} B^2 \delta_{ij}. \tag{2.35}$$

3. Magnetic forces in synchronous machines

In this chapter, a general description of magnetic forces in synchronous machines is presented. First, the concept of unbalanced magnetic pull and a technique to control the radial forces between the rotor and the stator of the machines are introduced. Second, a technique to influence the tangential forces that produce torque is presented. Finally, axial magnetic forces are discussed, magnetic thrust bearings are also introduced.

3.1 Radial forces

Faraday's law states that a voltage is induced in a coil with N number of turns that encloses a varying magnetic flux ϕ, according to:

$$V = -N\frac{d\phi}{dt}. \tag{3.1}$$

A synchronous generator can be broadly described by eq. (3.1). The voltage, V, is induced in the stator windings, usually three phase. They are constructed with N number of turns. The magnetic flux, ϕ, is typically provided by electromagnets. The torque that causes the electromagnets to rotate and, by consequence, provides the time variation of the flux $(d\phi/dt)$ in relation to the stator is provided by moving water, wind or steam. The rotating electromagnets, better known as *rotor poles*, ideally, provide an air gap magnetic flux density distribution according to:

$$B_i(\alpha) = \widehat{B}_i \cos(\alpha p). \tag{3.2}$$

Where the center of one of the rotor poles is aligned with the x axis, $\widehat{B}_i$ is the amplitude of the magnetic flux density, α is the azimuth angle, and p is the number of pole pairs. By integrating the magnetic pressure, as defined in eq. (2.23), along the rotor surface, the force between the rotor and the stator can be found. For any given machine with active length L and air gap radius R, the resulting forces between the rotor and the stator in the x and y directions are:

$$F_x = \int \sigma(\alpha)\cos(\alpha) RL d\alpha, \tag{3.3}$$

$$F_y = \int \sigma(\alpha)\sin(\alpha) RL d\alpha. \tag{3.4}$$

The force between a pole aligned with the x axis, and the stator can be found with the following equation:

$$F_p = \int_{-\frac{\pi}{2p}}^{\frac{\pi}{2p}} \sigma(\alpha)\cos(\alpha)RLd\alpha = \frac{2\widehat{B}_i^2 RLp^2 \sin(\frac{\pi}{2p})}{\mu_0(2p-1)(2p+1)}. \tag{3.5}$$

In an ideal machine, as shown in fig. 3.1, the magnitude of the force between each of the poles and the stator is identical. Due to symmetry, the flux density distribution described in eq. (3.2) results in zero net force between the rotor and the stator. This can also be found by integrating eqs. (3.3) and (3.4) around the whole circumference.

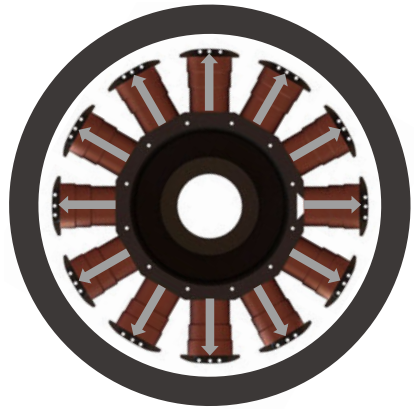

Figure 3.1. Magnetic force distribution in an ideal machine, the gray arrows illustrate force vectors.

In reality, no machine is ideal. There is always deviations that are caused for different reasons. For example: imperfect assembly, manufacturing tolerances, forced bending of the shaft, thermal expansion, non uniform cooling, stator segmentation, stator frame mechanical problems, shape form defects due to aging, inter turn short circuits in the rotor poles, alkali concrete growth, and floating rotor rings. If these imperfections lead to asymmetries in the magnetic flux density distribution, magnetic unbalance, there will be a resulting force between the rotor and the stator of the machine.

To illustrate the basic effect of these imperfections, please consider a machine with static eccentricity, as shown in fig. 3.2. The length of the air gap can be expressed as:

$$\delta_e(\alpha) = \delta_i(1 - \varepsilon\cos(\alpha - \theta_e)), \tag{3.6}$$

where δ_e and δ_i are the air gap lengths of the eccentric and the ideal machine, respectively. ε is the relative eccentricity, and θ_e the angular position of the shortest air gap. From eq. (3.6), a normalized and dimensionless function of the air gap permeance can be written as:

$$\lambda(\alpha) = \delta_i/\delta_e(\alpha) = 1/(1 - \varepsilon\cos(\alpha - \theta_e)). \tag{3.7}$$

If only the first two terms of a Maclaurin series are considered, eq. (3.7) can be expressed in the following form:

$$\lambda(\alpha) = (1 + \varepsilon \cos(\alpha - \theta_e)). \tag{3.8}$$

Therefore, the air gap flux density of a machine with static eccentricity is:

$$B_e(\alpha) = \lambda(\alpha) B_i. \tag{3.9}$$

By combining eq. (3.2) and eq. (3.8), the magnetic flux density of a machine with static eccentricity can be expressed as:

$$B_e(\alpha) = \widehat{B}_i \cos(\alpha p) + \widehat{B}_i \frac{\varepsilon}{2} \cos(\alpha(p+1) - \theta_e) + \widehat{B}_i \frac{\varepsilon}{2} \cos(\alpha(p-1) + \theta_e). \tag{3.10}$$

The resulting force in the direction of the shortest air gap (when $\theta_e = 0$) between the rotor and the stator of an eccentric machine caused by the magnetic flux density distribution described in eq. (3.10) becomes:

$$F_e = \int_0^{2\pi} \sigma(\alpha) \cos(\alpha) RL d\alpha = \frac{\widehat{B}_i^2 \varepsilon RL\pi}{2\mu_0}. \tag{3.11}$$

The first term in eq. (3.10) is the same flux density distribution as for the ideal machine, it results in zero net force. The second and third terms of eq. (3.10) are the air gap flux density harmonics [15, 72]. They are the cause of the resulting force shown in eq. (3.11). In fig. 3.2 the magnetic force vectors in each of the rotor poles of an eccentric machine are illustrated.

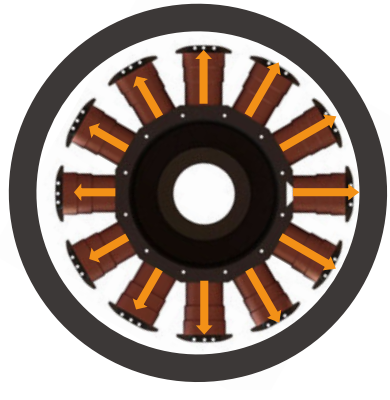

Figure 3.2. Magnetic force distribution in an machine with static eccentricity, the yellow arrows illustrate force vectors.

As an example, by inserting the data from table 3.1, in eq. (3.5), at $\widehat{B}_i = 1T$, the force between a single pole and the stator in the generator Porjus U9 is around $178.7kN$. The eccentricity force, according to eq. (3.11), at $\widehat{B}_i = 1T$ and $\varepsilon = 0.02$, is around $35.9kN$, at $\varepsilon = 0.10$, is around $179.8kN$.

Table 3.1. *Rotor dimensions, Porjus U9*

Number of pole pairs	5
Rotor radius	985 mm
Rotor length	1450 mm
Rotor weight	489.45 kN
Air gap length	15 mm

Control of radial magnetic forces

According to eq. (3.5), the force between a rotor pole and the stator of a synchronous machine is proportional to some geometrical constants (C) and the square of the magnetic flux density in the air gap, which in turn, according to eq. (2.21) is proportional to the electrical current for that particular electromagnet (I_p). With those equations in mind, the following can be concluded:

$$F_p = C\widehat{B_i}^2 = CI_p^2. \tag{3.12}$$

The relationship between the magnetic force and the electrical current can also be seen in eq. (2.18). From all these equations it can be concluded that by controlling the electrical current in each of the rotor poles the magnetic force between the rotor and the stator of a machine can be controlled. For machines with a large number of poles, a considerable amount of power electronics would be required.

In practice, from a magnetic force perspective, there is no need for individual pole control. The rotor field winding can be *split* and the rotor poles can be controlled in groups. Instead of magnetizing them as it is usually done, by applying the same field current I_f to all of them, an electrical current that has at least two parts is applied to each of the groups. The first part is a magnetizing component I_m, that fulfills the same purpose as the field current I_f. The second part is a sinusoidal component superposed on top of I_m with magnitude I_Δ, control angle α_c, and a phase angle that relates the spatial distribution of the currents and the pole groups. Please note that more than one sinusoidal component can be utilized, each at its own frequency.

In the following sections, two implementations are described. The first one with the rotor field winding *split* into three segments and the second with four segments.

Three segment implementation

Please consider the rotor of a 12 pole synchronous machine in which the field winding is *split* into three groups of 4 poles each. The magnetization of each group is controlled with respect to the other groups to create a controllable

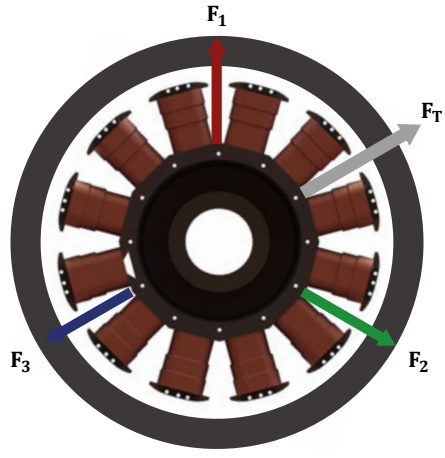

Figure 3.3. Magnetic forces in a rotor *split* in three segments.

force vector, $\mathbf{F_t}$. This is achieved by applying the following electrical currents, respectively to each group:

$$I_1 = I_m + I_\Delta \sin(\alpha_c), \tag{3.13}$$

$$I_2 = I_m + I_\Delta \sin(\alpha_c - \frac{2\pi}{3}), \tag{3.14}$$

$$I_3 = I_m + I_\Delta \sin(\alpha_c - \frac{4\pi}{3}). \tag{3.15}$$

From eq. (3.12), and the spatial distribution of the rotor pole groups as shown in fig. 3.3, the group forces can be expressed in term of Cartesian components:

$$\mathbf{F_1} = C I_1^2 \widehat{\boldsymbol{y}}, \tag{3.16}$$

$$\mathbf{F_2} = C\frac{\sqrt{3}}{2} I_2^2 \widehat{\boldsymbol{x}} - C\frac{1}{2} I_2^2 \widehat{\boldsymbol{y}}, \tag{3.17}$$

$$\mathbf{F_3} = -C\frac{\sqrt{3}}{2} I_3^2 \widehat{\boldsymbol{x}} - C\frac{1}{2} I_3^2 \widehat{\boldsymbol{y}}. \tag{3.18}$$

Where $\widehat{\boldsymbol{x}}$ and $\widehat{\boldsymbol{y}}$ are Cartesian unit vectors in the frame of reference of the rotor. The total force between the rotor and the stator is the sum of the force from each group:

$$\mathbf{F_t} = \mathbf{F_1} + \mathbf{F_2} + \mathbf{F_3}. \tag{3.19}$$

From eqs. (3.13) to (3.18), the components of the resultant force vector $\mathbf{F_t}$ in the direction of $\widehat{\boldsymbol{x}}$ and $\widehat{\boldsymbol{y}}$ are:

$$F_x = C\frac{\sqrt{3}}{2}(I_2^2 - I_3^2) = C\frac{\sqrt{3}}{4} I_\Delta (I_\Delta \sin(2\alpha_c) - 4 I_m \cos(\alpha_c)), \tag{3.20}$$

$$F_y = C(I_1^2 - \frac{1}{2}I_2^2 - \frac{1}{2}I_3^2) = C\frac{\sqrt{3}}{4}I_\Delta(4I_m\sin(\alpha_c) - I_\Delta\cos(2\alpha_c)), \tag{3.21}$$

and the magnitude of the resultant force, and its corresponding angle:

$$F_t = \frac{3}{4}|C||I_\Delta|\sqrt{I_\Delta^2 - 8I_mI_\Delta\sin(3\alpha_c) + 16I_m^2}, \tag{3.22}$$

$$\alpha_f = \tan^1\left(\frac{4I_m\sin(\alpha_c) - I_\Delta\cos(2\alpha_c)}{I_\Delta\sin(2\alpha_c) - 4I_m\cos(\alpha_c)}\right). \tag{3.23}$$

For a given magnetization level I_m, the force vector $\mathbf{F_t}$ can be controlled by adjusting I_Δ and α_c as required. When α_c is constant, the resulting force $\mathbf{F_t}$ rotates with the mechanical frequency, ω_m, of the machine, in the frame of reference of the stator. If a static vector is desired, for example to create a radial force or to counteract unbalanced magnetic pull, the control angle becomes $\alpha_c = \kappa - \omega_m t$, where t is the time, and κ is a constant.

To be able to apply the electrical currents described in eqs. (3.13) to (3.15), three single phase inverters can be utilized, one for each group. Another possibility is to connect the three segments of the rotor field winding in star and connect them to a three phase inverter as shown in fig. 3.4. The advantages of this implementation is that only half of the switches are required. The main disadvantage is that negative voltage cannot be applied to the field winding. In some cases, this can limit the control capabilities of the system. Another disadvantage is that even though there is three groups connected in star, four galvanic connections are needed between the *split rotor* and the power electronics because in this configuration $I_1 + I_2 + I_3 \neq 0$.

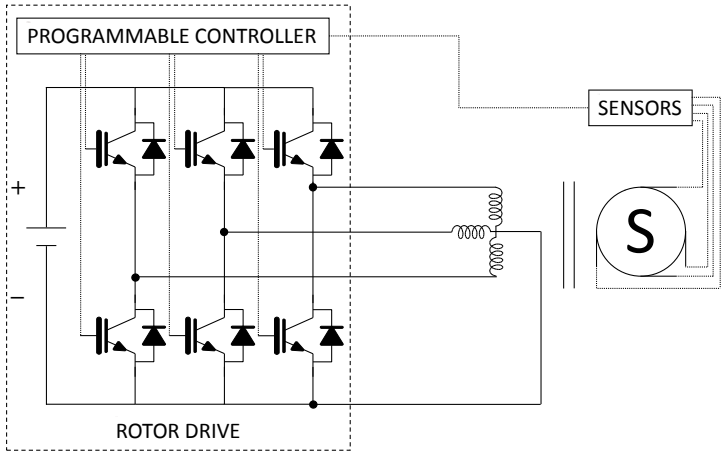

Figure 3.4. Power electronics required for a rotor *split* in three groups.

Four segment implementation

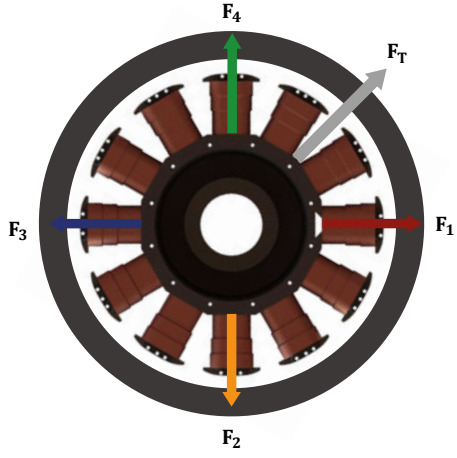

Figure 3.5. Magnetic forces in a rotor *split* in four segments.

For this implementation, please consider again the rotor of a 12 pole synchronous machine. This time, the field winding is *split* into four groups of 3 poles. In a similar way as for the three group implementation, the magnetization of each group is controlled with respect to the other groups to create a controllable force vector, $\mathbf{F_t}$. This is achieved by applying the following electrical currents, respectively to each group:

$$I_1 = I_m + I_\Delta \cos(\alpha_c), \tag{3.24}$$

$$I_2 = I_m + I_\Delta \cos(\alpha_c + \frac{\pi}{2}), \tag{3.25}$$

$$I_3 = I_m + I_\Delta \cos(\alpha_c + \pi), \tag{3.26}$$

$$I_4 = I_m + I_\Delta \cos(\alpha_c + \frac{3\pi}{2}). \tag{3.27}$$

From eq. (3.12), and the spatial distribution of the rotor pole groups as shown in fig. 3.5, the group forces can be expressed in term of Cartesian components:

$$\mathbf{F_1} = CI_1^2\widehat{\boldsymbol{x}}, \tag{3.28}$$

$$\mathbf{F_2} = -CI_2^2\widehat{\boldsymbol{y}}, \tag{3.29}$$

$$\mathbf{F_3} = -CI_3^2\widehat{\boldsymbol{x}}, \tag{3.30}$$

$$\mathbf{F_4} = CI_4^2\widehat{\boldsymbol{y}}. \tag{3.31}$$

Where $\widehat{\boldsymbol{x}}$ and $\widehat{\boldsymbol{y}}$ are Cartesian unit vectors in the frame of reference of the rotor. The total force between the rotor and the stator is the sum of the force from each group:

$$\mathbf{F_t} = \mathbf{F_1} + \mathbf{F_2} + \mathbf{F_3} + \mathbf{F_4}. \tag{3.32}$$

From eqs. (3.24) to (3.31), the components of the resultant force vector $\mathbf{F_t}$ in the direction of $\widehat{\boldsymbol{x}}$ and $\widehat{\boldsymbol{y}}$ are, respectively:

$$F_x = C(I_1^2 - I_3^2) = C4I_mI_\Delta\cos(\alpha_c), \tag{3.33}$$

$$F_y = C(I_4^2 - I_2^2) = C4I_mI_\Delta\sin(\alpha_c). \tag{3.34}$$

Therefore, the magnitude of the resultant force, and its corresponding angle are:

$$F_t = 4|C||I_\Delta||I_m|, \tag{3.35}$$

$$\alpha_f = \alpha_c. \tag{3.36}$$

For a given magnetization level I_m, the force vector $\mathbf{F_t}$ can be controlled by adjusting I_Δ and α_f as required. In a similar way as for a three segment implementation, when α_c is constant, the resulting force $\mathbf{F_t}$ rotates with the mechanical frequency, ω_m, of the machine, in the frame of reference of the stator. If a static vector is desired, for example to create a radial force or to counteract unbalanced magnetic pull, the control angle becomes $\alpha_c = \kappa - \omega_m t$, where t is the time, and κ is a constant.

To be able to apply the electrical currents described in eqs. (3.24) to (3.27), four single phase inverters can be utilized, one for each group. This would require eight galvanic connections between the *split rotor* and the power electronics. A better choice is to connect the four segments of the rotor field winding in star and connect them to a four phase inverter as shown in fig. 3.6. The advantages of this implementation is that half of the switches are required and that positive and negative voltage can be applied to the circuit. The main disadvantage is that half of the dc link voltage available is applied to each group because the rotor circuit is connected in star. This needs to be considered when determining the control capabilities required as described in section 2.6.

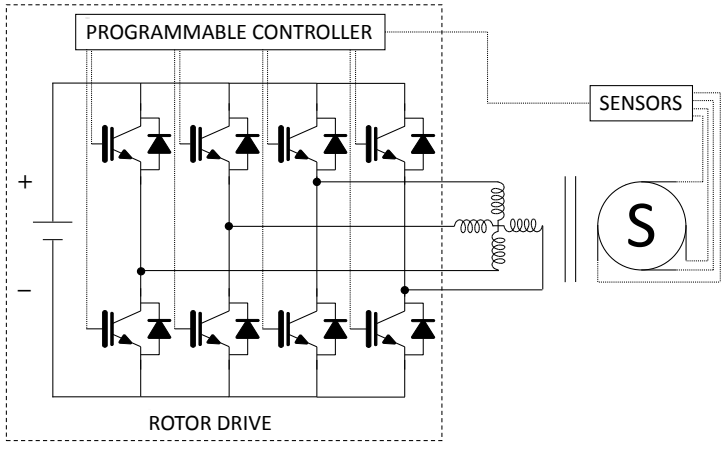

Figure 3.6. Power electronics for a rotor *split* in four segments.

3.2 Tangential forces

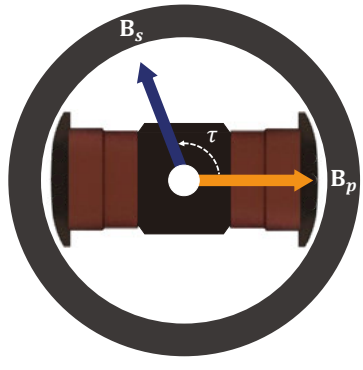

Figure 3.7. Flux vectors in a hypothetical two pole synchronous machine

Please consider a hypothetical synchronous machine, as shown in fig. 3.7. It has three phases, two identical rotor poles, it is perfectly centered, it has no damper bars, the effect of eddy currents and the inductance of the rotor winding can be neglected. Further, the rotor of this machine is locked, it is not allowed to rotate.

When voltage is applied to the stator terminals, the magnetic flux density contribution from the stator can be represented by a vector $\mathbf{B_s}$ that rotates at the line frequency in the frame of reference of the stator. The energized rotor contribute to the air gap flux density with a vector $\mathbf{B_p}$, aligned with the rotor poles. Since the rotor is locked, the frames of reference of the stator and the rotor are the same.

The torque vector $\mathbf{T}$ produced by the interaction between $\mathbf{B_s}$ and $\mathbf{B_p}$ in the air gap of the machine can be phenomenologically described by identifying

the rotor electromagnet as a magnetic dipole and considering the force on a magnetic dipole under the influence of an external field, according to the following equation:

$$\mathbf{T} = C(\mathbf{B_p} \times \mathbf{B_s}) = C|\mathbf{B_p}||\mathbf{B_s}|\sin(\tau)\widehat{\boldsymbol{z}}. \tag{3.37}$$

Where C is a constant related to the dimensions and construction of the machine, τ is the angle between the vectors $\mathbf{B_p}$ and $\mathbf{B_s}$, and $\widehat{\boldsymbol{z}}$ is a unit vector perpendicular to the plane of the flux vectors, positive in the direction of the reader.

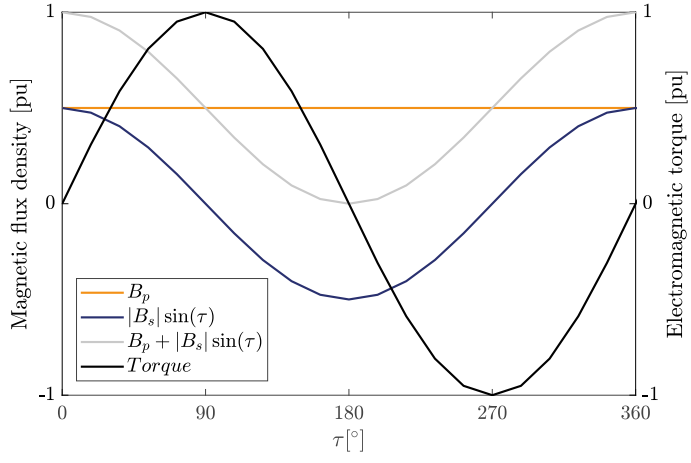

Figure 3.8. Electromagnetic torque and magnetic flux density in front of one of the rotor poles when the rotor polarity is constant.

As $\mathbf{B_s}$ rotates, the rotor experiences positive torque and negative torque as shown in fig. 3.8. In the same figure, the total air gap flux density in front of one of the rotor poles is shown as well as the flux density contributions from $\mathbf{B_s}$ and $\mathbf{B_p}$.

The polarity of the rotor poles decides the direction of the vector $\mathbf{B_p}$ with respect to the rotor, which in turn, as it can be seen in eq. (3.37), affects the direction of $\mathbf{T}$. By controlling the polarity of the rotor poles, the resulting torque on the machine can be affected. By inverting the polarity of the rotor field at the peaks of the stator flux density, $|\mathbf{B_s}|\sin(\tau)$, relative to the rotor poles, maximum torque is achieved. This is shown in fig. 3.9.

With the technique described in this section, braking and accelerating torques can be achieved. It can be useful, for example, to create a starting torque. During start, as the machine accelerates, the relative frequency between vectors $\mathbf{B_s}$ and $\mathbf{B_p}$ reduces until the vectors are synchronous. A possible implementation of the power electronics required is shown in fig. 3.10

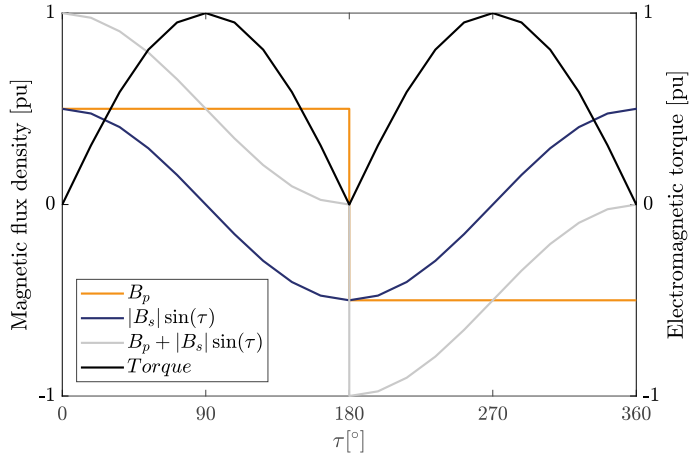

Figure 3.9. Electromagnetic torque and magnetic flux density in front of one of the rotor poles when $\mathbf{B_p}$ is inverted at the peaks of $|\mathbf{B_s}|\sin(\tau)$.

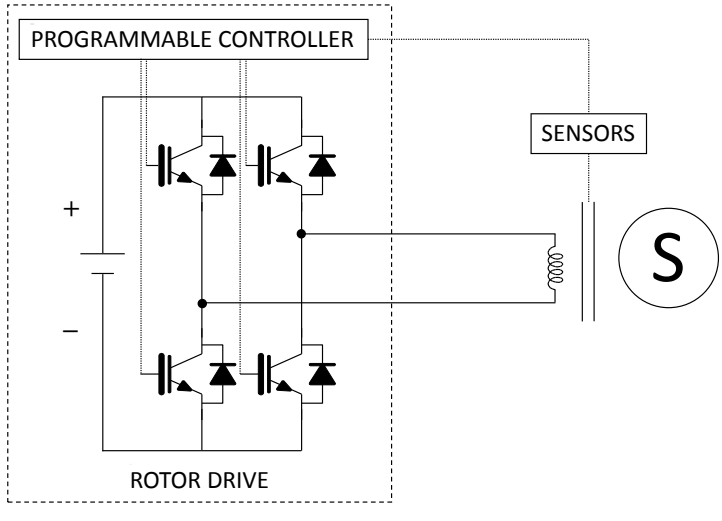

Figure 3.10. Power electronics required to invert the polarity of the rotor field.

3.3 Axial forces

The magnets inherent to the operation of the synchronous machines are provisioned to generate tangential forces, as shown in section 3.1 they can be used to create radial forces as well.

When it comes to axial forces in a synchronous machine, Marcusson has shown that leakage, particularly when the rotor and stator are not centered in the axial position, can provide thrust [73]. The use of this effect has been proposed and successfully utilized for other types of electrical machines in applications that do not require high axial stiffness [74–76], for example in centrifugal blood pumps [77].

However, for synchronous machines, the force due to axial leakage has a relatively small magnitude and stiffness, creates additional losses, and when not centered axially, the output voltage of a generator is reduced, in the case of a motor, the torque. Moreover, the magnitude of the axial force is dependant on the current in the rotor, controlling it would interfere with the control of the magnetization of the machine. Therefore, to create axial magnetic forces in a synchronous machine, a dedicated axial actuator is required. In the following sections two types of magnetic thrust bearings are introduced.

Electromagnetic thrust bearings

An electromagnetic thrust bearing is in essence an electromagnet with a rotating target. When a constant load is applied, the theory described in sections 2.4 and 2.5, regarding their force capabilities is applicable. This limitation is because it is hard to laminate an electromagnetic thrust bearing, therefore the effect of the Eddy currents that appear during dynamic loading can not be neglected.

In a laminated electromagnet, the speed at which the force can be controlled, also known as bandwidth is limited by the inductance and the resistance of the circuit. In a non laminated structure, Eddy currents also play a role. When the frequency of the current applied to the electromagnet terminals increases, the resultant force is proportionally reduced until at some point it becomes negligible, a phase lag is also introduced [78]. There are analytical methods available to calculate the influence of Eddy currents in solid actuators [79, 80]. The finite element method can also be utilized.

If required, the influence of Eddy currents can be reduced by introducing cuts in the core [81], resulting in an improvement of the dynamic performance of the actuator. However, there are not only drawbacks with them. In some cases, not being able to change the flux rapidly, and by consequence the force, can be utilized as an advantage.

Please consider a large vertical machine in which an electromagnetic thrust bearing has been installed as a thrust compensator for a conventional hydrodynamic bearing. In case of an unexpected power interruption to the magnetic

bearing, the energy stored in the inductance provides a soft discharge of the magnetic bearing. If designed properly, in a non laminated structure, it is not physically possible to extract the energy relatively fast, even if the controller tries to do it, due to the influence of the Eddy currents. This feature adds reliability to the system.

An schematic of a possible implementation of the power electronics and sensors for a magnetic thrust bearing utilized as a thrust compensator is shown in fig. 3.11

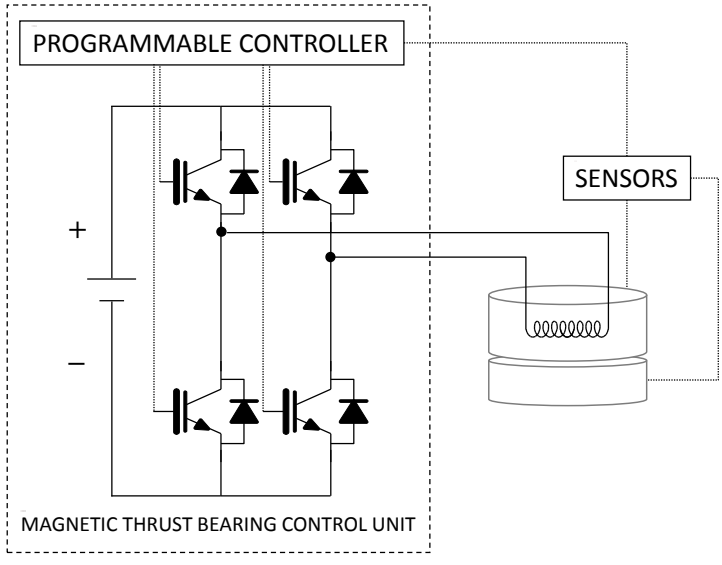

Figure 3.11. Magnetic thrust bearing control unit.

For reference, the area of the magnetic thrust bearing for the synchronous generator Porjus U9 is 1.77 m^2. It can carry in total 1450 kN. At maximum load, the average pressure is around 0.8 MPa. The rotor weight is nearly 490 kN and the maximum water load is 960 kN.

Permanent magnet thrust bearings

Bearings constructed with permanent magnets can be utilized either in repulsive or attractive mode, many different topologies exist. To explore the building blocks of one of the topologies, please consider three permanent magnets as shown in fig. 3.12 (Left). The magnetic flux lines, naturally, follow the magnetization of the permanent magnets. If the magnet in the center is positioned in between the other two instead, as shown in fig. 3.12 (Right), most of the magnetic flux lines are redirected from one side of the assembly into the other. This results in an increase of flux on one side and, ideally, to the cancellation of flux on the other. This construction is known as a Halbach array. To

create repulsive forces, two of them can be utilized. The magnetic field distribution for a two dimensional Halbach array can be found analytically [82]. It can be also utilized as an approximation of three dimensional arrays [83]. For large assemblies, finite element is preferred. As it will be shown in section 4.1, Halbach arrays can be used as permanent magnet thrust bearings.

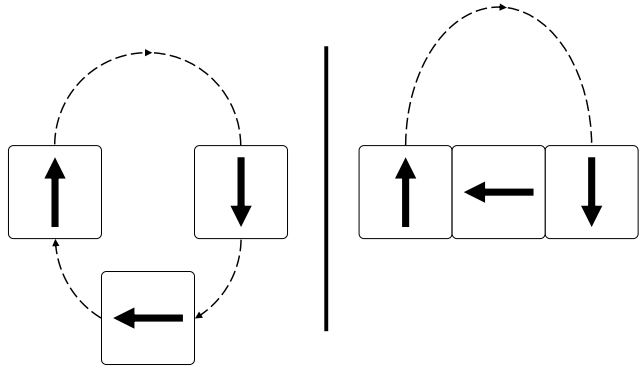

Figure 3.12. (Left) Three permanent magnets. (Right) Halbach array assembly.

Part II:
Experimental work

4. Experimental test rig

4.1 Overview

All the work presented in this thesis has been validated experimentally. Most of the equipment utilized has been designed and constructed by fellows at the Division of the Electricity. The most laborious and time consuming task among those presented in this thesis was the upgrade of the experimental test rig. A photo after the upgrade is shown in fig. 4.1. The main components are numbered in fig. 4.2 and described in table 4.1.

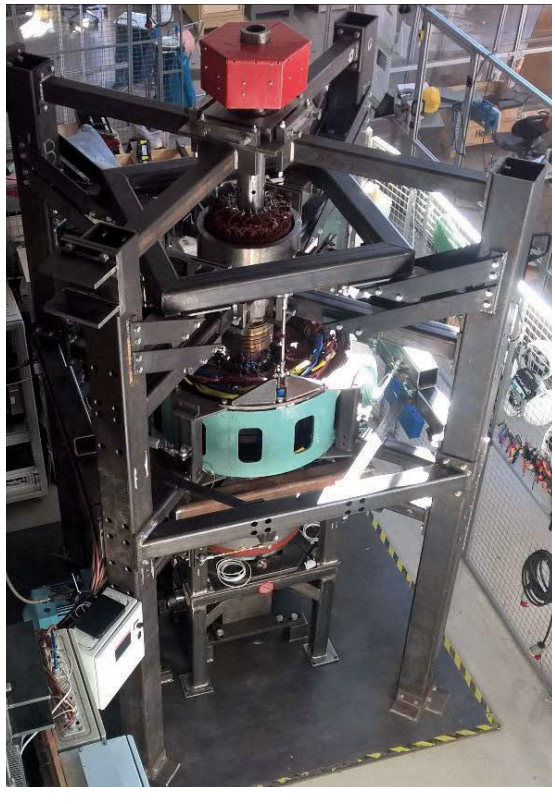

Figure 4.1. Synchronous machine test rig.

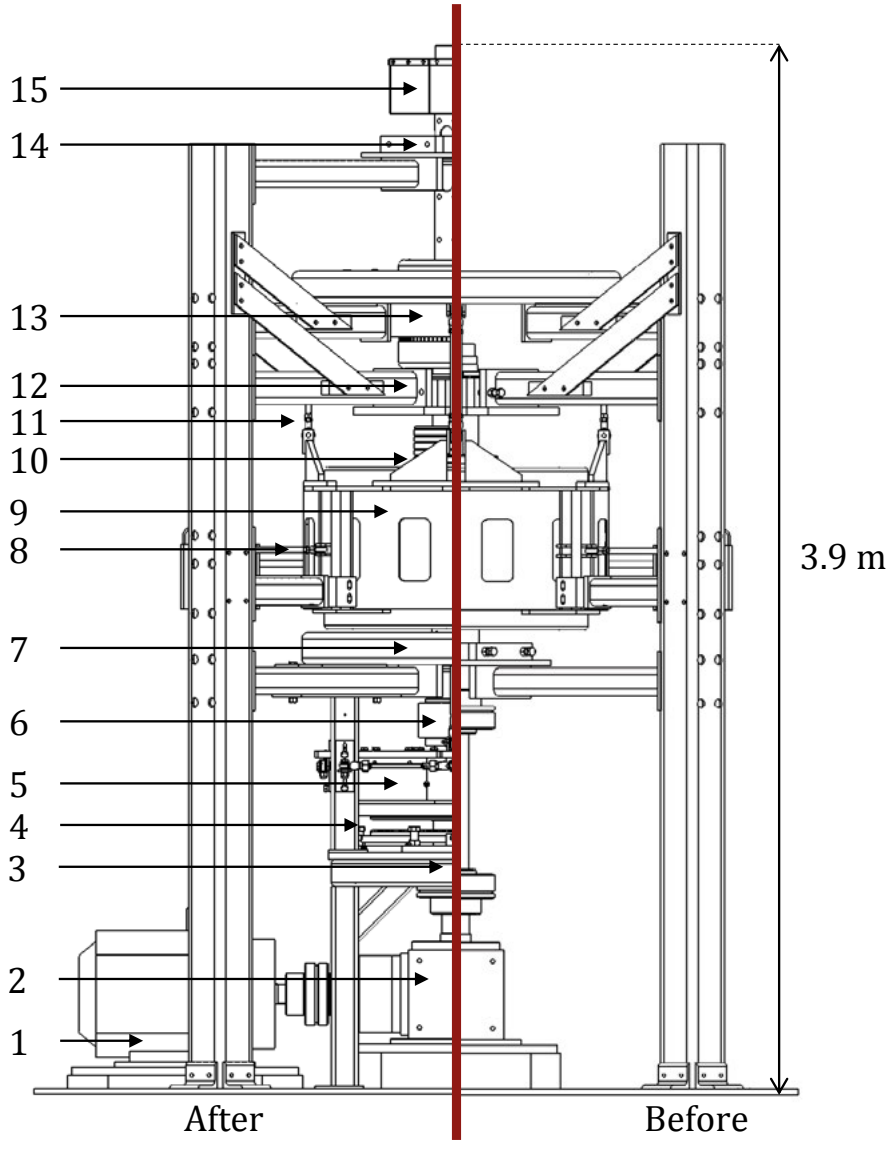

Figure 4.2. Schematic of the test rig before and after the upgrade.

Table 4.1. *Major components of the synchronous machine test rig*

Number	Component
1	Induction machine
2	Gearbox
3	Ball spline
4	Permanent magnet thrust bearing
5	Electromagnetic thrust bearing
6	Radial magnetic bearing rotor
7	Radial cylindrical roller bearing
8	Radial support bar
9	Synchronous machine
10	Slip rings
11	Axial support bar
12	Axial cylindrical roller bearing
13	Permanent magnet brushless exciter
14	Radial roller bearing
15	Rotating power electronics

Induction Machine, flexible couplings, gearbox and ball spline
The induction machine utilized in the test rig has four poles, it is rated 55 kW, the model is M2AA250SMB4. When used as a motor it is driven by an ACS8000100703, both are from ABB. The right angle gearbox has a gear ratio of 3:1. It is a Z75ASM6 from STM SpA. There are two flexible couplings in the rig, one that connects the induction machine with the gearbox and another one that couples the gearbox with the main shaft. Both are Centaflex model CF-A-140. The steel hub of the top coupling was machined by electrical discharge to fit the spline shaft directly in the hub. A picture the result can be seen in fig. 4.3. The outer race of the ball spline is a 50.8 mm (2 inch), 6 races model 7828135. The inner race, is a 381 mm (15 inch) spline shaft model 5706436, both from Thomson linear. The assembly is installed on the bore of the main shaft as shown in fig. 4.3. A ball spline was utilized to allow axial adjustment of the shaft.

Figure 4.3. Ball spline and flexible coupling.

Permanent magnet thrust bearing
The permanent magnet thrust bearing is assembled by hand from 2532 Nd-Fe-B, N48, 12 mm cubic magnets supplied by Sura Magnets. There are 1279 pieces in the rotor and 1253 in the stator. There are two magnets less in each stator row. The purpose is to achieve a better overlap of magnetic material across the array despite the segmentation. The magnets are installed in 26 concentric rows of magnets, 13 in the rotor and 13 in the stator. They form Halbach arrays that are homopolar in the direction of rotation. The magnets are mounted on plates of steel grade S235JR. To be able to position all of them in the right place, 2 polycarbonate meshes were watercut with the assembly pattern and used as a guide. Each magnet was glued to the steel plate and

the polycarbonate mesh either with Loctite 496, and/or Loctite 326 with 7649 primer. Afterwards both, the rotor and stator, were casted in epoxy with resin RenLam® M-1 and hardener Ren® HY 956. The stator is mounted on a table with adjustable height, three load cells, model LTH 350 from Futek, are installed between the stator and the table. When it is set to the lowest position, the shaft rest on the mechanical thrust bearing. As it is adjusted upwards, the permanent magnet thrust bearing starts unloading the mechanical bearing. In the highest position, the permanent magnet thrust bearing takes all the load. Photos of the bearing during assembly are shown in fig. 4.4

Figure 4.4. Permanent magnet thrust bearing during assembly.

Electromagnetic bearings
The electromagnetic thrust bearing installed in the test rig is a modified version of a one degree of freedom bearing arrangement with integrated passive electrodynamic dampers [84]. It was designed by T. Lembke. Allegedly, passive damping is provided in an efficient way at very high speeds. However, at relative low speeds, like the case of this test rig, active control is a better choice.

In this design, the stator is segmented into three identical sections. The coils that feed each section can be energized independently. The rotor and stator areas that face the air gap are provided with a teethed structure. The purpose of this construction is to create radial forces as well as thrust by controlling the magnetization in each bearing segment and exploiting the radial leakage flux caused by the teethed structure. Photos of one of the stator segments are shown in fig. 4.5

The amount of radial force achieved with such a construction is very low. Moreover, due to the teethed structure, the overall size of the electromagnet increases considerably compared to a traditional actuator, for example a C core designed for the same axial force. Therefore, in synchronous machines, it is better to use a dedicated actuator for the axial thrust. A thorough analytical and experimental investigation of the magnetic forces due to radial and axial fluxes in teethed structures is published by Walowit and Albrecht [85, 86].

The test rig is also prepared for a future radial magnetic bearing. The rotor target is already installed.

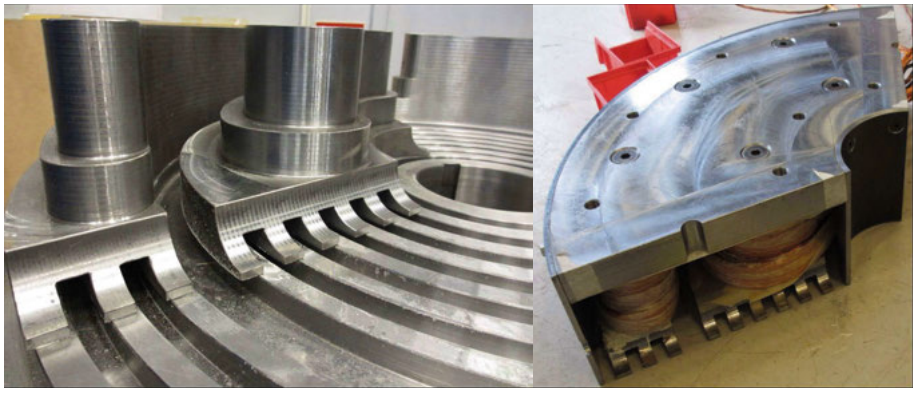

Figure 4.5. Electromagnetic thrust bearing stator segment during assembly.

Cylindrical roller bearings
There is two radial cylindrical roller bearings in the test rig. The inner races are NU 2326 ECMA, they have a height of 93 mm, while the outer races are NU 326 ECP, with a height of 58 mm. All from SKF. The height difference between the inner and outer races allow axial adjustment of the shaft. The mechanical thrust bearing is a cylindrical roller bearing model 89430-M from INA. In fig. 4.6, a photo of one of the radial bearing assemblies with the bearing block and supporting plate can be seen as well as the rollers of the mechanical thrust bearing.

Figure 4.6. Radial and thrust roller bearings during assembly.

Permanent magnet brushless exciter and rotating power electronics
The test rig is equipped with a permanent magnet brushless exciter that can be connected either in a six phase or a three phase configuration. There are two interchangeable sets of rotating power electronics. The first one is a thyristor based current sourced converter. It can be used in either six or twelve pulse configuration. To control the thyristors, a FC36M firing board from United Automation is used for the three phase connection. For the six phase, an FC36M auxiliary firing board is also used as a slave. This set of power electronics has been tested extensively [87–89], but never under rotation. In fig. 4.7 photos of the thyristor based rectifying box and the core of the exciter during assembly are shown.

The second set is a voltage sourced converter [90]. The rectification side of the converter has diodes. The inverting side has eight MOSFET switches that can be utilized for a three or four segment *split rotor* implementation as described in section 3.1. To control the switches, a programmable automation controller with a Bluetooth interface is provided [91]. The system has been fully tested statically and for mechanical integrity under rotation.

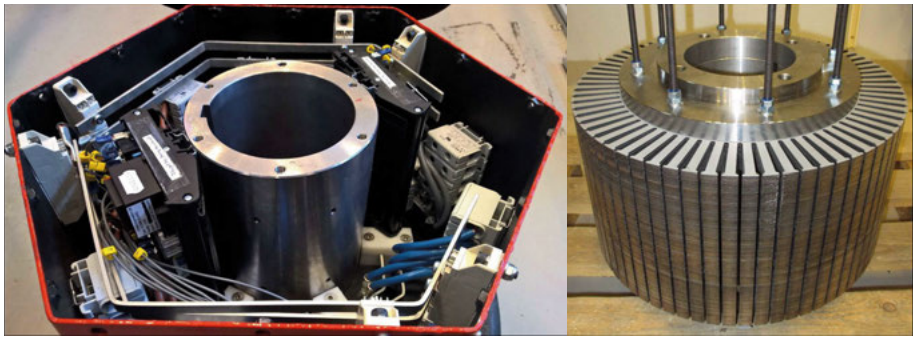

Figure 4.7. Box with thyristors and exciter rotor during assembly.

Slip rings and power electronics.
The test rig is provided with six slip rings. They can be utilized to feed the rotor poles either from a DC supply, a three phase thyristor based current sourced converter, or a six phase IGBT based voltage sourced converter. The DC supply utilized is an EA-PS8160-170 from Elektro-Automatik, it is also used to feed the DC link of the six phase IGBT based voltage sourced converter. In the inverting side of the converter, two three phase IGBT stacks from Powerex, model PP200T120-ND are used. The control is provided from a programmable automation controller that sits in the aluminum box shown in fig. 4.8. For the three phase thyristor based current sourced converter, a FC36M firing board from United Automation is utilized, the firing angle is set using a potentiometer. Photos of the slip rings, the voltage sourced converter and the current sourced converter can be seen in fig. 4.8.

Figure 4.8. Slip rings, IGBT based voltage sourced converter and thyristor based current sourced converter.

Synchronous machine and support bars
The main component of the test rig is a 12 salient pole synchronous machine. Originally, it was utilized as a motor to test turbines. It was donated to the University by GE Hydro. The stator winding, originally single circuit, has been modified. Today it is possible to connect it either as single circuit or as two parallel circuits [38]. The rotor, originally with solid poles, has been modified as well. Laminated pole shoes and a removable damper cage have been installed [9, 92]. Photos taken during the early days of construction of the test rig can be seen in fig. 4.9. The stator and of one of the rotor poles before being wound are shown. Please note that these modifications were made before the author was part of the Division of Electricity.

Figure 4.9. Stator and rotor of the synchronous machine.

The rotor shaft is held in place by the radial bearings, ideally it should not move in the radial direction. The axial position of the rotor can be adjusted by moving the stator of the permanent magnet thrust bearing. The stator hangs from eight support bars, four radial and four axial. Each bar is attached to the stator and the test rig structure with ball joints. Moreover, the length of the bars can be adjusted. With this configuration, the stator can be positioned

as desired. This flexibility allows the study of the machine while eccentric, axially and radially. All the bars have strain gauges installed. To measure the strain and condition the signal, amplifiers can be connected to the gauges [93] as shown in fig. 4.10.

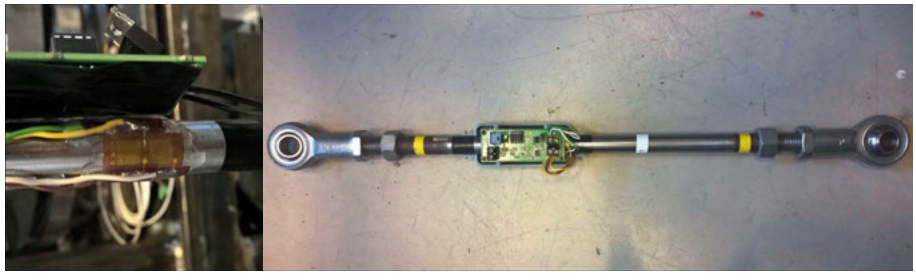

Figure 4.10. Strain gauge, support bar and amplifying circuit.

Magnetic flux sensors
Besides the strain gauges, the test rig is equipped with more than one hundred sensors. Of particular interest for this thesis are the magnetic flux sensors [91]. Twenty four of them are installed in the rotor, two for each pole. In the stator, there are four of them, ninety degrees apart from each other. Photos of the installed flux sensors during the assembly of the test rig can be seen in fig. 4.11

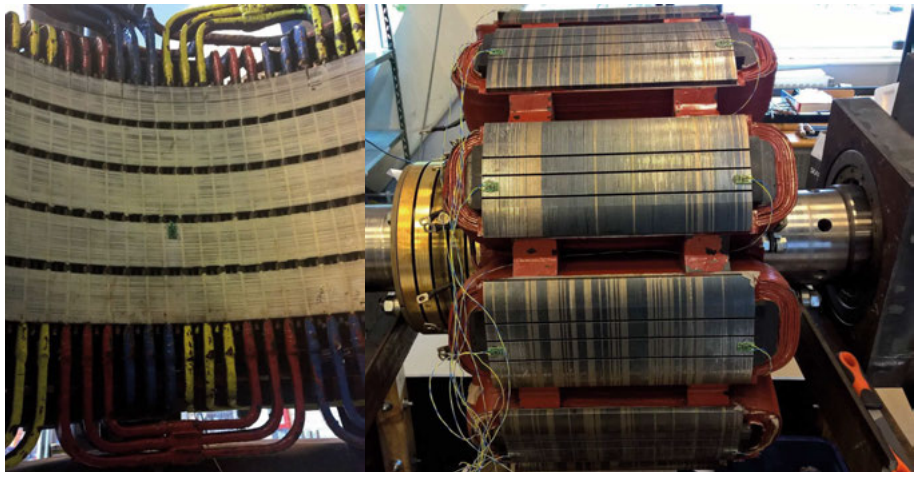

Figure 4.11. Magnetic flux sensors in the stator and rotor of the synchronous machine.

5. Full scale demonstrations

In Porjus, a small village situated along the Lule river a few steps from the Laponian area, a UNESCO World Heritage site, there are two hydropower stations. The *new station*, among the largest in Sweden, has two units that are rated 267 MVA, and the historical *old station*, that has two 10 MW units. Together with Olidan, in the Göta river, and Älvkarleby in the Dal river, Porjus is among the pioneer hydropower stations in the country [94].

Since 1994, the *old station* is also the host of the Porjus hydropower centre, originally an initiative between Vattenfall, ABB Generation, and Kvaerner Turbine is today, operated by a foundation owned by Vattenfall, GE Hydro and Andritz. Besides being a museum, the Porjus hydropower centre is a non commercial site with an operational hydropower station dedicated to training, research and development. The old G8 and G9, were replaced by new machines. U8 with a Francis turbine, and U9 with a Kaplan turbine [95]. U8 has been utilized for development and training, while U9 has been used, by and large, to develop and test new technology [96]. U9, commissioned in 1998, is the first Powerformer ever built [97, 98]. At present day, the technologies proposed in this thesis, are being demonstrated in U9. The rotor field winding is already segmented and a magnetic thrust bearing is in place.

The value that such a centre has for the Swedish hydropower industry can be estimated not only in terms of the human capital it provides through education and training. Before being established, it was calculated that an increase of 1% in efficiency, a reduction of 10% in investment costs, and a reduction of 10% in operation and maintenance, has an economical value of 2 billion Swedish crowns over a period of 30 years [96, 99].

Today, more than 20 years after its foundation, and in light of the challenges that an aging fleet faces, the Porjus hydropower centre continues to offer unique possibilities for education, training, research, and development.

Figure 5.1. The *old station*, called the temple in the wilderness [100], and the *new station* [101].

5.1 Control of radial magnetic forces in Porjus U9

Hydropower equipment is expected to last for decades. However, it is not time that determines the lifetime of the mechanical components in a machine, it is the number of load cycles it is subjected to [102]. In a period of 40 years, the number of load cycles due to mechanical and magnetic unbalance in a hydropower generator ($> 10^7$) is a few orders of magnitude larger than other load spectra components, for example: the number of start and stop operations (2 per day=28,800 cycles) or the number of load rejections (3600). That is why, it is very important to keep the radial loads caused by magnetic unbalance well bellow the fatigue limit [6]. Further, according to a corporate report sponsored by EPRI, New England Power Co., New York Power Authority and Seattle City Light, in some cases, magnetic unbalance can lead to stator winding fault from mechanical abrasion of the stator insulation system even before failure of the rotor rim [103].

The *split rotor* technology has the potential to extend the lifetime of hydropower generators by improving the load spectra components that lead to mechanical fatigue in the unit. That is the motivation to add a *rotor drive* to Porjus U9 and demonstrate the technology in full scale. For example: during start and stop cycles radial forces can be created to optimize the load in the radial bearings, during operation and load rejection the magnitude of radial forces caused by magnetic unbalance can be kept to a minimum. With a *rotor drive*, new machines are spared from unnecessary wear and tear. In older machines, during refurbishment, more mechanical components can be kept for longer time, thus reducing the expenditure. Even though, from a Swedish perspective, U9 is relatively small in terms of generating capacity, the nominal rotor magnetizing current is 810 A, representative for the generators used in the hydropower industry.

As it can be seen from the photos in fig. 5.2, the rotor field winding of U9 is already *split*, the rotor drive is under construction. Initial tests are expected by the end of this year.

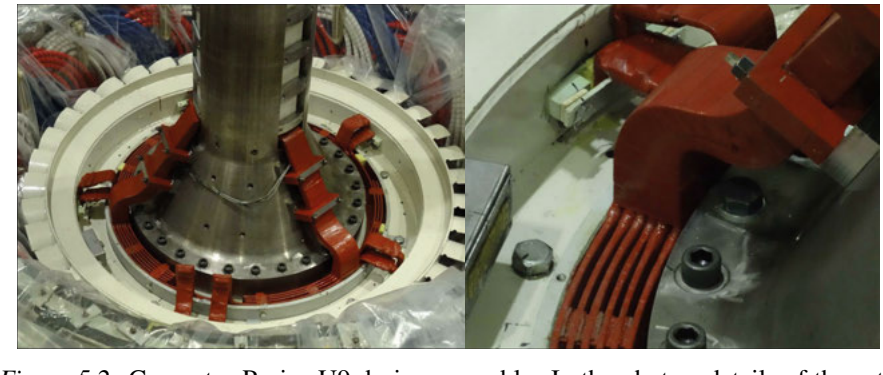

Figure 5.2. Generator Porjus U9 during assembly. In the photos, details of the rotor winding connections are shown.

5.2 Magnetic thrust bearing for Porjus U9

The thrust bearing is an important component in hydropower units, it carries the load of the rotating parts of the generator as well as the water load. Typically, tilt pad bearings are utilized. The losses in a thrust bearing, are highly dependant on its radius, therefore the bearing should be as small as possible [53]. The design of the bearing is a compromise between the allowable pressure in the bearing pads and the mean sliding speed of the sliding thrust bearing area. An increase in bearing area results in lower pressure, but in higher sliding speed. Therefore, the only way to reduce the thrust bearing losses is either to allow a higher pressure, or reduce the thrust [55].

The motivation to install a magnetic thrust bearing, or thrust compensator in a hydropower unit, is that by reducing the thrust on the mechanical thrust bearing pads, the technology has proven to increase the reliability, reduce the losses and starting torque in the machines [104]. Moreover, the need for thrust bearing auxiliary equipment, such as oil pumps and cooling equipment is reduced. With less pressure in the mechanical thrust bearing pads, there is a possibility to change the lubrication, typically mineral oil, to an environmentally friendly version. These reasons lead to the installation of a magnetic thrust bearing in Porjus U9, the first of its kind in Sweden.

General information about some magnetic thrust bearings utilized in power stations with vertical axis synchronous machines, including Porjus U9, can be found in table 5.1 [58, 60, 61, 64, 65, 104].

Table 5.1. *Magnetic thrust bearing installations in power plants*

Power Plant	Country	Year	Machine type	Total thrust (ton)	Magnetic thrust (ton)	Load reduction %
Porjus*	SWE	2017	**Kaplan**	148	145	**98**
Dinorwig*	GBR	2001	Reversible Francis	520	200	38
Yamazaki	JPN	1996	Francis	14	FL**	FL**
Palmiet	ZAF	1988	Reversible Francis	924	458	50
Samrangjin	KOR	1983	Reversible Francis	1230	590	48
Chongpyong	KOR	1978	Reversible Francis	580	250	43
Midono	JPN	1965	Francis	672	315	47
Kuromatagawa No. 2	JPN	1963	Deriaz	300	102	34
Hatanagi No. 1	JPN	1961	Reversible Francis	493	244	49
Wadagawa No. 2	JPN	1958	**Pelton**	240	202	**84**
Tochio	JPN	1956	**Pelton**	78	62	**79**
Motosu	JPN	1956	**Pelton**	32	27	**84**
Shin-Sapporo	JPN	1955	**Synchronous condenser**	38	145	**90**
Muroran	JPN	1955	**Synchronous condenser**	42	38	**90**
Fuji Electric Co.	JPN	<1964	**Laboratory Generator**	130	125	**96**

Notes: *Only one unit in the station has a magnetic thrust bearing. **Full levitation.

From table 5.1, it can be seen that a high percentage of load reduction, more than 79%, has been achieved only in machines in which the axial dynamics are relatively slow (Pelton turbines, condensers, laboratory equipment). If the operational tests are successful, the magnetic thrust bearing for Porjus U9, which is equipped with a Kaplan turbine, will be the exception. In the laboratory, it has been concluded that the magnetic thrust bearing for Porjus U9 is able to take the maximum load in the unit, even during fast transients such as load rejection. This was achieved by designing the actuator with an in house finite element program taking into consideration the required maximum load, allowable size, rate of thrust change, the stiffness of the mechanical thrust bearing including the bearing bracket, as well as the stiffness of the foundation of the magnetic thrust bearing. A photo of the magnetic thrust bearing installed in Porjus U9 can be seen in fig. 5.3.

Figure 5.3. Magnetic thrust bearing in Porjus U9.

6. Experiments

6.1 Radial forces

Two measurement campaigns have been performed in the experimental test rig to evaluate the performance of the *split rotor* system.

The first one was with a three segment implementation as described in section 3.1. In this campaign, three sets of measurements were performed. In the first one, the machine was centered as well as possible. In the second round, static eccentricity of around 25% was introduced. Finally, with the rotor relatively well centered, an inter turn short circuit was simulated by connecting a resistor in parallel with one of the rotor poles. All these experiments were performed at 1/3 of rated speed, no load. The machine was driven with the induction motor through the gearbox. Measurements of magnetic flux in the stator and rotor, magnetization currents and strain were recorded with and without active compensation of unbalanced magnetic pull.

The second campaign was with a four segment implementation as described in section 3.1. One set of measurements was performed with static eccentricity of 20%. The experiments were performed at rated speed, no load. In a similar way as for the first campaign, the induction motor was used as a prime mover. Measurements of damper bar currents and magnetizing currents were recorded with and without active compensation of unbalanced magnetic pull.

6.2 Tangential forces

To demonstrate that tangential forces can be influenced to produce accelerating torques in a synchronous machine, the technique described in section 3.2 was implemented in the experimental test rig. The stator was feed from a three phase voltage sourced converter, a *rotor drive* was installed as shown in fig. 3.10. During this campaign, the machine was accelerated from standstill to synchronization and also operated asynchronously. Measurements of flux and magnetizing current were recorded.

6.3 Axial forces

Permanent magnet thrust bearing

To evaluate the performance of the permanent magnet thrust bearing described in section 4.1, measurements of axial force, axial force ripple and spin down

tests have been performed. To evaluate the axial force that the permanent magnet bearing can produce, the rotor of the assembly was pulled mechanically towards the stator. Measurements of the resulting force between both parts were recorded with load cells, the distance was measured manually with a caliper. To evaluate the axial force ripple, force measurements were recorded during rotation at rated speed using load cells. The relative position between the rotor and the stator was also measured and recorded using a high accuracy Eddy current sensor model eddyNCDT3010,S2 from MICRO-EPSILON. Finally, two spin down tests were performed. On one test the machine was resting on the permanent magnet thrust bearing, and on the other one it was resting on the mechanical thrust bearing. On both tests, the machine was accelerated to 1/3 of the rated speed, afterwards the prime mover was turned off. Measurements of rotational speed were recorded as the machine decelerated.

Magnetic thrust bearing for Porjus U9

So far, only laboratory tests and dry tests of the magnetic thrust bearing for Porjus U9 have been performed.

In the laboratory, two measurement campaigns were performed. In the first one, solid washers with a height of 5 mm were inserted between the rotor and the stator. In this condition, measurements of magnetic flux in relation to the DC current applied to the terminals of the magnetic thrust bearing were recorded. It was also verified that the force rate of change achieved is fast enough to clear load rejection. Further, the amount of axial force obtained in relation to the application of sinusoidal currents to the magnetic thrust bearing terminals (bandwidth) was measured up to 10 Hz. Finally, the power consumption of the magnetic thrust bearing for different magnetization levels, including the control unit were measured.

During the second campaign, 72 Belleville washers were inserted between the rotor and the stator of the magnetic thrust bearing. Their stiffness and the reaction force they produce when compressed, are of the same order of magnitude as Porjus U9. With this setup, dynamic tests were performed.

During the dry tests, correct function of the sensors (position sensors and load cells) was verified. Further, the magnetic thrust bearing force was increased gradually, at the same time measurements of the axial position of the magnetic thrust bearing rotor relative to its stator were recorded. The axial deflection of the foundation were the stator is mounted, at two different locations, was measured and recorded as well. With these sets of measurements, the stiffness of different structural elements in the construction was evaluated.

Part III:
Findings

7. Summary of results

Active compensation of unbalanced magnetic pull is achieved for static eccentricities as large as 25%, during no load at rated speed, with three and four segment implementations.

Active compensation of unbalanced magnetic pull is achieved for inter turn short circuits, during no load at rated speed, with a three segment implementation.

It is shown that during active compensation of unbalanced magnetic pull, eccentricity harmonics are heavily reduced, indicating magnetic balance.

It is shown that magnetic balance leads to higher electromagnetic efficiency.

It is shown that with active compensation of unbalanced magnetic pull, the currents in the damper bars are reduced. Further, it is shown that with individual pole control they can be nearly eliminated. The induced currents due to slot ripple persist.

It is shown that with active compensation of unbalanced magnetic pull, the currents in the parallel circuits are eliminated when the span of a stator circuit is larger than a rotor segment.

It is demonstrated that by inverting the rotor polarity with respect to the stator field, a laminated salient pole synchronous machine can be started without the need of damper bars.

It is shown that utilization of permanent magnet thrust bearings for rotor weights in the orders of tons is technically feasible.

It is shown that the utilization of electromagnetic thrust bearings in hydropower units with fast dynamics such as Kaplan turbines is technically feasible.

It is shown that the size of the power electronics pack of the magnetic thrust bearing control unit is reduced compared with similar systems.

8. Conclusions

Three different technologies to control magnetic forces in synchronous machines have been presented. One technology for each, radial, tangential and axial forces.

With the first technology, by controlling the radial forces in the machine, magnetic balance is achieved. Further, radial forces can be created to positively affect the rotordynamic behaviour of the machines. These improvements translate in a reduction of the mechanical loads the machine and structure have to endure, resulting in increased robustness towards structural strength and fatigue, leading to reduced maintenance and increased machine lifetime.

With the second technology, it has been demonstrated that by magnetizing the rotor in innovative ways, tangential forces can be influenced. The implication is that braking and accelerating torques can be created. Therefore, it is possible to start a synchronous machine and operate it asynchronously, utilizing power electronics on the rotor side, rather than using auxiliary motors, damper cages, or power electronics in the stator, which are usually considerably larger. In hydropower units, this can be utilized during start operations to accelerate the machine electrically rather than with water in order to spare the turbine from wear. With the elimination of damper bars, this technology increases the competitiveness of small and medium size synchronous machines in the high efficiency motor segment.

With the third technology, by using magnetic thrust bearings designed for dynamic loads and paired with modern power electronics and controllers in combination with mechanical thrust bearings, satisfactory dynamic performance can be achieved even for units with Kaplan turbines, resulting in a more efficient and robust thrust bearing system.

9. Future work

The users of synchronous machines for hydropower specify allowable levels of machine eccentricity during commissioning. Standards for allowable levels of magnetic unbalance in terms of resulting forces, similar to mechanical balancing standards should also be considered.

The functionality of the *split rotor* to eliminate magnetic unbalanced has been demonstrated. Its use to improve further mechanical balancing grades should be investigated.

On the rectifying side of a current controlled voltage sourced converters used to excite a synchronous machine, as in the case of the *rotor drive*, low current comes into the capacitors to overcome the losses in the system. On the inverting side, a high current is sustained through the inductance of the winding. Therefore, as opposed to the use of current sourced converters, a magnetizing transformer is not required to reach the high current that the excitation requires. The main reason to use a magnetizing transformer then, is galvanic isolation. However, the fact that the converter is current controlled reduces the risk of high current flow, should a ground fault occur. Therefore, the avoidance of a magnetizing transformer when a machine is excited with a current controlled voltage sourced converter should be considered.

With static excitation systems, the *split rotor system* requires four galvanic connections to the rotor winding. The utilization of maintenance free rolling rings instead of slip rings and brushes should be investigated.

Extensive work has been performed in parallel on the *split rotor* system when utilized with a *rotor drive* connected to the machine via slip rings, and on brushless exciters with rotating electronics. Motor start capabilities have been demonstrated as well. All research can converge in the development of a rotating *rotor drive*. Such a device should include motor start and magnetic balance capabilities.

With the work presented in this thesis, the reasons to utilize a damper cage in some applications of synchronous machines can be questioned. For example, in a synchronous generator, the damper cage performs the following tasks: damping of torque oscillations, reduction of parasitic air gap magnetic field harmonics, suppression of the negative sequence field at unbalanced load operation, protection of the excitation winding at transient faults, transient stability, and asynchronous start up [105]. The functionality that the damper

cage provides, can be replaced with power electronics connected to the rotor. The possibilities of highly efficient laminated synchronous machines without damper cages should be explored further.

The magnetic bearing control unit presented in this work, requires an order of magnitude less current when compared to similar systems. This results in considerable economic savings due to the reduction of the power electronics package. Further reduction of the power electronics required should be investigated.

With the addition of a magnetic thrust bearing in a hydropower unit, the pressure in the mechanical bearing pads can be reduced considerably. Therefore, the requirements of the lubricant used in the mechanical thrust bearing are less severe. The use of environmentally friendly substitutes for the lubricating oil should be explored in order to improve the sustainability of the thrust bearing system.

Summary of papers

Paper I

Optimization of force between cylindrical permanent magnets
In this letter, a comparison of the optimal dimensions with respect to magnetic force for two coaxial cylindrical permanent magnets is presented. The exercise is performed for different permanent magnet materials as well as for ideal permanent magnets. The purpose is to illustrate the importance of modelling permanent magnets correctly with respect to material properties. The results are validated with measurements. The author was involved in all aspects of the work. Particularly on the analytical calculations, finite element calculations and data analysis.
Published in IEEE Magnetics Letters, vol. 5, pp. 1-4, October 2014.

Paper II

Simple method to calculate the force between thin walled solenoids
In this paper, a method to calculate the axial force between concentric thin walled solenoids is presented. The purpose of the work is to simplify the calculations of force by circumventing the use of elliptical integrals. The results are validated against existing analytical solutions, finite element simulations and measurements. The author was involved in all aspects of the work. Particularly on the method and its validation.
Published in Progress in Electromagnetics Research M, vol. 51, pp. 93-100, October 2016.

Paper III

Demonstration of active compensation of unbalanced magnetic pull in synchronous machines
In this article, active compensation of unbalanced magnetic pull in a synchronous machine is demonstrated. Full compensation was achieved for 25% static eccentricity as well as for inter turn rotor short circuits. The technology was implemented with a *split rotor* into three segments. The author was involved in all aspects of the work except finite element simulations and control programming.
Published in CIGRE Science & Engineering, vol. 8, pp. 98-107, June 2017.

Paper IV

Electromagnetic losses in synchronous machines during active compensation of unbalanced magnetic pull due to static eccentricity
In this publication, the electromagnetic losses during active compensation of unbalanced magnetic pull in a synchronous machine are calculated. Finite element simulations are validated with damper bar current measurements in an experimental test rig. Afterwards, simulations for a large machine are performed. The technology was implemented with a *split rotor* into four segments. The author was involved in all aspects of the work except finite element simulations and control programming.
Accepted for publication in IEEE Transactions on Industrial Electronics.

Paper V

Arrangement and method for force compensation in electrical machines
In this patent, an electrical machine with: a stator, at least one sensor and a rotor that has: rotor windings, a power supply, and a magnetization control arrangement is disclosed. A method for controlling such an electrical machine is also disclosed. The author is one of the inventors.
Published by the Swedish patent and registration office, Patent specification SE 538 502 C2.

Paper VI

Demonstration of synchronous motor start by rotor polarity inversion
In this letter, it is communicated that it is possible to start a synchronous motor by inverting the polarity of the rotor field with respect to the rotating stator field. The technique is validated in a test rig. Further, finite element simulations for a 20 MVA machine are presented. The author was involved in all aspects of the work except finite element simulations and control programming.
Accepted with revisions in IEEE Transactions on Industrial Electronics.

Paper VII

Synchronous machine and method for operating a synchronous machine
In this patent application, methods and devices for providing a more efficient control of a synchronous machine during periods of varying rotor speed are disclosed. The author is one of the inventors.
To be published by the Swedish patent and registration office, Patent Application SE 175 0223-8.

Paper VIII

Construction of a permanent magnet thrust bearing for a hydropower generator test setup

In this conference article, the mechanical construction and some aspects of the design of a permanent magnet thrust bearing for a vertical axis synchronous machine test rig are described in detail. The author was involved in all aspects of the work.

Presented by the author at the 1st Brazilian Workshop on Magnetic Bearings.

Paper IX

Magnetic modeling and measurement of forces between permanent magnet rings used as passive magnetic bearings

This conference contribution was written in cooperation with colleagues from Universidade Federal do Rio de Janeiro in Brazil. For this work, two arrays of permanent magnets utilized as magnetic bearings were constructed. The force between the magnets was measured and simulated using the finite element method. In the finite element simulations, different linear models of the magnetic properties were utilized. The author was involved in all aspects of the work except the radial bearing simulations and measurements.

Presented by the author at the 1st Brazilian Workshop on Magnetic Bearings.

Paper X

Initial performance tests of a permanent magnet thrust bearing for a hydropower synchronous generator test-rig

In this conference article, initial tests performed on the permanent magnet thrust bearing constructed for a vertical synchronous machine test rig are presented. The article was completed taking into consideration the feedback received during the conference. Afterwards, it was submitted and accepted for publication in ACES Journal. The author was involved in all aspects of the work.

Presented by the author at Advances in Magnetics, AIM 2016.

Paper XI

Performance tests of a permanent magnet thrust bearing for a hydropower synchronous generator test-rig

In this contribution, the results of measurements performed on a permanent magnet thrust bearing designed and constructed for an experimental test rig are presented. The thrust measurements are compared with three dimensional finite element simulations. The author was involved in all aspects of the work. Particularly on the design, construction, and assembly of the magnetic thrust bearing as well as in the finite element simulations.

Accepted for publication in ACES Journal

Paper XII

Magnetic thrust bearing for a hydropower unit with a Kaplan turbine

In this work, laboratory, commissioning, and performance tests on a magnetic thrust compensator installed in the generator Porjus U9 will be reported. The author is involved in all aspects of the work except finite element simulations and control programming.

Unpublished manuscript.

Paper XIII

Arrangement for supporting a rotatable body, EP16196073

In this patent application, an arrangement for supporting a rotatable body comprising a magnetic thrust bearing, and a system comprising such arrangement are disclosed. The objective of such arrangement and system is to minimize the size of the air gap of a magnetic thrust bearing. For a repulsive permanent magnet thrust bearing, this is achieved by installing the stator of the magnetic thrust bearing in a structure with lower stiffness than the bearing itself. With this arrangement, when the bearing is loaded, the air gap remains substantially constant. The author is one of the inventors.

To be published by the European Patent Office, Patent application EP16196073.

Paper XIV

Fail-safe system for discharging a magnetic thrust bearing, EP16200156

In this patent application, a fail safe system and a method for discharging a magnetic thrust bearing is disclosed. The objective of the disclosures is to maintain safe operation of the installation even in the case of component failure at all times, including load rejection in a hydropower plant. The author is one of the inventors.

To be published by the European Patent Office, Patent application EP16200156.

Paper XV

Passive axial thrust bearing for a flywheel energy storage system
In this conference paper, results of the evaluation of two different permanent magnet thrust bearings constructed for a high speed flywheel are presented. Measurements of thrust were performed and compared with finite element simulations. Further, the electromagnetic losses were evaluated with the finite element method. The work presented in this contribution was refined and published in the International Journal of Applied Electromagnetics and Mechanics. The author had a minor role in this contribution.
Presented by M. Hedlund at the 1st Brazilian Workshop on Magnetic Bearings.

Paper XVI

Eddy currents in a passive magnetic axial thrust bearing for a flywheel energy storage system
In this article, two types of permanent magnet thrust bearings designed and constructed for a high speed flywheel are evaluated regarding their thrust capabilities and eddy current losses. Measurements of thrust were performed and compared with finite element simulations. Further, the electromagnetic losses were evaluated with the finite element method. The work presented in this contribution is a revised and refined version of an article presented at the 1st Brazilian Workshop on Magnetic Bearings. The author had a minor role in this contribution.
Published in the International Journal of Applied Electromagnetics and Mechanics, vol. 54, no. 3 pp. 389-404, July 2017.

Paper XVII

Analysis of passive magnetic bearings for kinetic energy storage systems
This conference paper was written in cooperation with colleagues from Universidade Federal do Rio de Janeiro, Universidade Federal Fluminense, and Universidade Federal de Juiz de Fora, all of them in Brazil. In the paper, a passive magnetic bearing system consisting of a permanent magnet radial bearing and an axial superconducting magnetic bearing is described. The bearings were tested independently, results of the measurements are reported. The author had a minor role in this contribution.
Presented by J. de Santiago at the 14th International Symposium on Magnetic Bearings.

Paper XVIII

Passive magnetic bearing system

This conference contribution was written in cooperation with colleagues from Universidade Federal do Rio de Janeiro, Universidade Federal Fluminense, and Universidade Federal de Juiz de Fora, all of them in Brazil. In the article, a passive magnetic bearing system consisting of a permanent magnet radial bearing and an axial superconducting magnetic bearing is described. Static and dynamic tests were performed for the magnetic bearing system. Results of the measurements are reported. The author had a minor role in this contribution.

Presented by E. Rodriguez at the 22nd International Conference on Magnetically Levitated Systems and Linear Drives.

Paper XIX

Design and characterization of a rotating brushless PM exciter for a synchronous generator test setup

In this conference article, the design and construction of a permanent magnet brushless exciter for a vertical synchronous machine test rig is presented. The author was involved in the construction and installation of the exciter and the measurements.

The article was presented by J. Nøland at the XXII International Conference of Electric Machines.

Paper XX

Evaluation of different power electronic interfaces for control of a rotating brushless PM exciter

In this conference paper, the performance of three different power electronics topologies utilized to rectify the output of a permanent magnet brushless exciter are investigated. The author was involved in the construction of the equipment utilized, in the measurements, and in the discussion around the different topologies utilized.

The paper was presented by J. Nøland at the 42nd annual Conference of the IEEE Industrial Electronics Society.

Paper XXI

Design and characterization of a rotating brushless outer pole PM exciter for a synchronous generator

This is an extension of the paper presented at the XXII International Conference of Electric Machines. In this article, a review of exciter technologies and a general design methodology of a permanent magnet brushless rotating exciter are presented. Static tests of a thyristor based current sourced converter connected to the permanent magnet brushless exciter via slip rings are also presented. The author was involved in the construction and installation of the exciter, in the design and construction of the thyristor based current sourced converter, as well as in the measurements.

The paper is published in IEEE Transactions on Industry Applications, vol. 53, no. 3, pp. 2016-2027, May 2017.

Paper XXII

Testing of active rectification topologies on a six-phase rotating brushless outer pole PM exciter

In this paper, voltage sourced converters and current sourced converters used to rectify the output of a six, or three phase permanent magnet brushless exciter for a synchronous machine test rig are examined. The benefits and drawbacks of the topologies are discussed. The author was involved in the construction and installation of the exciter, in the design and construction of the thyristor based current sourced converter, in the measurements and in the discussion around the different topologies.

Accepted with revisions in IEEE Transactions on Energy Conversion.

Paper XXIII

Comparison of thyristor rectifier configurations for a six-phase rotating brushless outer pole PM exciter

In this article, 12 pulse thyristor based current sourced converters used to rectify the output of a six phase permanent magnet brushless exciter are discussed. The converter can be utilized either in series or parallel connection of two three phase systems. Benefits and drawbacks of both configurations are identified. Further, the use of a hybrid system that combined the benefits of both topologies is proposed. The author was involved in the construction and installation of the exciter, in the design and construction of the thyristor based current sourced converter, and in the discussion around the different topologies.

Accepted for publication in IEEE Transactions on Industrial Electronics.

Svensk sammanfattning

Magnetiska krafter utgör en fundamental del av en synkronmaskin. Radiella, tangentiella samt axiella krafter förekommer under drift. I den här avhandlingen presenteras tre olika teknologier som använder sig av dessa krafter.

Den första teknologin utnyttjar de radiella krafter som uppstår mellan rotor och stator under drift. Detta görs genom ett nytt koncept i vilket fältlindningens poler delas upp i grupper vilka magnetiseras individuellt, med målsättningen att utöka systemets kontrollerbara frihetsgrader. Denna teknologi gör det möjligt att balansera den elektriska maskinen magnetiskt, vilket resulterar i avsevärda förbättringar i dess rotordynamiska beteende. Det är även möjligt att använda de radiella krafterna på andra sätt, exempelvis för att motverka krafter som uppstår på grund av gravitationen. Detta koncepts tekniska genomförbarhet har visats i laboratoriet. Den första fullskaliga installationen har redan påbörjats i Porjus vattenkraftverk, i norra Sverige.

Den andra teknologin innefattar kontroll av magnetiseringsfältet för att påverka de tangentiella krafter som producerar vridmoment. Detta mål nås genom att invertera polariteten på strömmen i fältlindningen som funktion av positionen hos magnetfältet som produceras av armaturlindningen. Teknologin gör det möjligt att skapa vridmoment som bromsar eller accelererar den elektriska maskinen genom att kontrollera rotorströmmen. Detta är speciellt användbart för att starta en synkronmotor. Denna teknologi har visats i laboratoriet.

Rotorn och statorn i en synkronmotor använder sig av de tangentiella krafter som skapas genom interaktionen mellan deras respektive magnetfält. Det har visats att även de radiella krafter som skapas kan användas. De axiella krafter som skapas under drift, emellertid, är försumbara. För att skapa axiella krafter är det därför fördelaktigt att använda sig av ett system speciellt utformad för detta ändamål, ett axiellt magnetiskt lager. Målet är att, tillsammans med det axiella mekaniska lagret, öka effektiviteten samt pålitligheten hos maskinen. Denna teknologi har använts under ett flertal årtionden i ett fåtal vattenkraftstationer. I denna avhandling presenteras en uppdatering av denna teknologi. Ett axiellt magnetiskt bärlager har installerats i vattenkraftverket i Porjus för att visa på dess fördelar.

Arbetet som presenteras i denna avhandling har utförts vid Uppsala Universitet, institutionen för teknikvetenskaper, avdelningen för elektricitetslära. Det baseras på ny forskning som använder sig av analytiska beräkningar, datorsimulationer och ett extensivt experimentellt arbete. Under arbetets gång har jag fått ett ovillkorligt stöd från min familj, mina vänner och mina kollegor. För detta är jag djupt tacksam.

Resumen en español

Las fuerzas magnéticas son inherentes a las máquinas síncronas. Durante su operación, se presentan fuerzas radiales, tangenciales y axiales. Es esta tesis, se propone el uso de tres tecnologías diferentes para utilizar estas fuerzas.

Con la primer tecnología se logra el aprovechamiento de las fuerzas radiales que aparecen entre el rotor y el estator de las máquinas durante su operación. Esto mediante un nuevo concepto, en el cual el devanado de campo es dividido en grupos de polos, que a su vez son magnetizados independientemente con el objeto de añadir grados de control al sistema. Con dicha tecnología, es posible balancear las máquinas magnéticamente, lo que resulta en considerables mejoras a su comportamiento rotor dinámico. Es posible también utilizar las fuerzas radiales para otros propósitos, por ejemplo, contrarrestar el efecto de la gravedad. La factibilidad técnica de dicho concepto ha sido probada en el laboratorio. La primer instalación a gran escala, puesta ya en marcha, será en una de las unidades de la estación hidroeléctrica Porjus, en el norte de Suecia.

La segunda tecnología implica el control del campo de magnetización con el objeto de influenciar las fuerzas tangenciales que producen torque. El objetivo se logra invirtiendo la polaridad del devanado de campo con respecto a la posición instantánea del campo magnético que resulta de la armadura. Con esta nueva técnica, es posible crear momentos de frenado y aceleración en la máquina controlando el rotor. Es particularmente útil durante el arranque de un motor síncrono. Dicha tecnología ha sido demostrada en el laboratorio.

En una máquina síncrona, el rotor y el estator están dispuestos para hacer uso de las fuerzas tangenciales que resultan de la interacción de sus campos magnéticos. Ha sido demostrado que también se puede hacer uso de las fuerzas radiales. Cuando se trata de fuerzas axiales, las resultantes entre el rotor y el estator durante la operación de una máquina síncrona, son despreciables. Por esto, para crear fuerzas axiales útiles es recomendable utilizar un actuador provisto para ello, un balero de carga magnético, axial. El objetivo de hacerlo, es en conjunto con el balero mecánico, incrementar la eficiencia y confiabilidad de la máquina. Dicha tecnología ha sido utilizada durante décadas en algunas estaciones hidroeléctricas. En esta tesis, se presenta una actualización de dicha tecnología. Con el objetivo de demostrar las mejoras, se ha instalado un balero magnético axial en una de las unidades de la estación hidroeléctrica Porjus.

El trabajo presentado en esta tesis ha sido llevado a cabo en la Universidad de Uppsala, dentro del Departamento de Ciencias de la Ingeniería de la División de Electricidad. Está basado en investigación original sustentada

con cálculos analíticos, simulaciones computacionales y extenso trabajo experimental. Durante este esfuerzo, he recibido el soporte incondicional de mi familia, amigos y colegas por lo que estoy profundamente agradecido.

Acknowledgements

The work presented in this thesis has been carried out at Uppsala University. In this quest I have been supported by my friends and colleagues from the Division of Electricity to whom I am deeply grateful.

Special thanks to my supervisor Urban Lundin for his trust and advice over the years, to Niklas Dahlbäck, and Johan Bladh for their invaluable support, to my assistant supervisors Mats Leijon, and Thommy Karlsson for their insight, to Arne Wolfbrandt for his expertise, and to my colleagues in the hydropower group, C. Johan D. Abrahamsson, Fredrik Evestedt, Jonas K. Nøland, Mattias Wallin, Martin Fregelius, Martin Ranlöf, Weijia Yang, Linn Saarinen, Birger Marcusson, and Per Norrlund for their engagement and enthusiasm.

For their help with the experimental test rig Tobias Kamf, Kerstin Lindström, Tomas Johnson, Lucas Reis Conceição, Paulo César Ribeiro, Igor Lima de Paula, Yasmin Monteiro Cyrillo, Hugo Biccas Valente, Gustavo Fernandes Oliveira, Ulf Ring, Dana Salar, Juan de Santiago, Markus Gabrysch, Joel Weissbach, Maciej Kawecki, and Linda Ekmarker, are also acknowledged.

For their support with the full scale installations at Porjus Billy Kjäll, Henrik Lundström, Peter Eriksson, Håkan Olsson, Ulf Björklund, and Stig-Arne Jansson deserve to be mentioned.

Further, my appreciation to Helena Ströberg, Mats Wahlén, Pedro Vicente Jover Rodriguez, Lars-Erik Kämpe, and Bo Hernnäs for their advice.

Finally, my grattitude to Vattenfall, SweGRIDS, The Swedish Energy Agency, STandUP for energy, Uppsala University Innovation, Uppsala Innovation Centre, InnoEnergy, ALMI, Vinnova, Conacyt, Ångström Materials Academy, and Ingeniería de Control y Potencia for their support.

References

[1] G. Neidhofer, "The evolution of the synchronous machine," *Engineering Science and Education Journal*, vol. 1, pp. 239–248, Oct 1992.

[2] A. Gray and J. G. Pertsch, "Critical review of the bibliography on unbalanced magnetic pull in dynamo-electric machines," *Transactions of the American Institute of Electrical Engineers*, vol. XXXVII, pp. 1417–1424, July 1918.

[3] R. E. Hellmund, "Series vs. parallel windings for a. c. motors," *Electrical World*, vol. 49, pp. 388–389, Oct 1907.

[4] L. Lundström, R. Gustavsson, J. O. Aidanpää, N. Dahlbäck, and M. Leijon, "Influence on the stability of generator rotors due to radial and tangential magnetic pull force," *IET Electric Power Applications*, vol. 1, pp. 1–8, January 2007.

[5] E. Rosenberg, "Magnetic pull in electric machines," *Transactions of the American Institute of Electrical Engineers*, vol. XXXVII, pp. 1425–1469, July 1918.

[6] M. Nässelqvist, R. Gustavsson, and J. O. Aidanpää, "A methodology for protective vibration monitoring of hydropower units based on the mechanical properties," *Journal of dynamic systems, measurement, and control*, vol. 135, no. 4, p. 041007, 2013.

[7] R. Gustavsson, *Rotor dynamical modelling and analysis of hydropower units*. PhD thesis, Luleå tekniska universitet, 2008.

[8] M. Nässelqvist, *Simulation and characterization of rotordynamic properties for vertical machines*. PhD thesis, Luleå tekniska universitet, 2012.

[9] M. Wallin, *Measurement and modelling of unbalanced magnetic pull in hydropower generators*. PhD thesis, Acta Universitatis Upsaliensis, 2013.

[10] M. Karlsson, *Modelling and analysis of multiphysical interactions in hydropower rotor systems*. PhD thesis, Luleå tekniska universitet, 2008.

[11] N. Lundström, *Dynamic consequences of shape deviations in hydropower generators*. PhD thesis, Luleå tekniska universitet, 2006.

[12] Y. Calleecharan, *Contributions to the electromechanics of unbalanced magnetic pull in a synchronous hydropower generator*. PhD thesis, Luleå tekniska universitet, 2013.

[13] D. Žarko, D. Ban, I. Vazdar, and V. Jarica, "Calculation of unbalanced magnetic pull in a salient-pole synchronous generator using finite-element method and measured shaft orbit," *IEEE Transactions on Industrial Electronics*, vol. 59, pp. 2536–2549, June 2012.

[14] M. Michon, R. C. Holehouse, K. Atallah, and G. Johnstone, "Effect of rotor eccentricity in large synchronous machines," *IEEE Transactions on Magnetics*, vol. 50, pp. 1–4, Nov 2014.

[15] P. V. Jover-Rodriguez, A. Belahcen, A. Arkkio, A. Laiho, and J. A. Antonino-Daviu, "Air-gap force distribution and vibration pattern of induction

motors under dynamic eccentricity," *Electrical engineering*, vol. 90, no. 3, pp. 209–218, 2008.
[16] D. G. Dorrell, J. K. H. Shek, and M. F. Hsieh, "The development of an indexing method for the comparison of unbalanced magnetic pull in electrical machines," *IEEE Transactions on Industry Applications*, vol. 52, pp. 145–153, Jan 2016.
[17] A. Belahcen and A. Arkkio, "Computation of additional losses due to rotor eccentricity in electrical machines," *IET Electric Power Applications*, vol. 4, pp. 259–266, April 2010.
[18] A. Sinervo, *Effects of slotting and unipolar flux on magnetic pull in a two-pole induction motor with an extra four-pole stator winding*. PhD thesis, Aalto University, 2013.
[19] A. Burakov, *Modelling the unbalanced magnetic pull in eccentric-rotor electrical machines with parallel windings*. PhD thesis, Helsinki University of Technology, 2007.
[20] T. P. Holopainen, *Electromechanical interaction in rotordynamics of cage induction motors*. PhD thesis, VTT Technical Research Centre of Finland, 2004.
[21] A. Tenhunen, *Electromagnetic forces acting between the stator and eccentric cage rotor*. PhD thesis, Helsinki University of Technology, 2003.
[22] A. Laiho, *Electromechanical modelling and active control of flexural rotor vibration in cage rotor electrical machines*. PhD thesis, VTT Technical Research Centre of Finland, 2009.
[23] P. V. Jover-Rodríguez, *Current-, force-, and vibration-based techniques for induction motor condition monitoring*. PhD thesis, Helsinki University of Technology, 2007.
[24] B. Silwal, *Power Balance in the Finite Element Analysis of Electrical Machines*. PhD thesis, Aalto University, 2017.
[25] A. Belahcen, *Magnetoelasticity, magnetic forces and magnetostriction in electrical machines*. PhD thesis, Helsinki University of Technology, 2004.
[26] M. Nässelqvist, R. Gustavsson, and J. O. Aidanpää, "Bearing load measurement in a hydropower unit using strain gauges installed inside pivot pin," *Experimental mechanics*, vol. 52, no. 4, pp. 361–369, 2012.
[27] D. G. Dorrell, A. Salah, and Y. Guo, "The detection and suppression of unbalanced magnetic pull in wound rotor induction motors using pole-specific search coils and auxiliary windings," *IEEE Transactions on Industry Applications*, vol. 53, pp. 2066–2076, May 2017.
[28] D.-H. Hwang, S.-B. Han, B.-C. Woo, J.-H. Sun, D.-S. Kang, B.-K. Kim, and Y.-H. Cho, "Detection of air-gap eccentricity and broken-rotor bar conditions in a squirrel-cage induction motor using the radial flux sensor," *Journal of Applied Physics*, vol. 103, no. 7, p. 07F131, 2008.
[29] J. Flugestad, "Measurements of magnetic flux density in rotating machines," Master's thesis, University of Agder, 2014.
[30] A. J. Ellison and S. J. Yang, "Effects of rotor eccentricity on acoustic noise from induction machines," *Electrical Engineers, Proceedings of the Institution of*, vol. 118, pp. 174–184, January 1971.
[31] J. R. Cameron, W. T. Thomson, and A. B. Dow, "Vibration and current

monitoring for detecting airgap eccentricity in large induction motors," *IEE Proceedings B - Electric Power Applications*, vol. 133, pp. 155–163, May 1986.
[32] C. Bruzzese and G. Joksimovic, "Harmonic signatures of static eccentricities in the stator voltages and in the rotor current of no-load salient-pole synchronous generators," *IEEE Transactions on Industrial Electronics*, vol. 58, pp. 1606–1624, May 2011.
[33] C. Bruzzese, "Diagnosis of eccentric rotor in synchronous machines by analysis of split-phase currents;part i: Theoretical analysis," *IEEE Transactions on Industrial Electronics*, vol. 61, pp. 4193–4205, Aug 2014.
[34] C. Bruzzese, "Diagnosis of eccentric rotor in synchronous machines by analysis of split-phase currents;part ii: Experimental analysis," *IEEE Transactions on Industrial Electronics*, vol. 61, pp. 4206–4216, Aug 2014.
[35] M. Wallin, J. Bladh, and U. Lundin, "Damper winding influence on unbalanced magnetic pull in salient pole generators with rotor eccentricity," *IEEE Transactions on Magnetics*, vol. 49, pp. 5158–5165, Sept 2013.
[36] M. Karlsson, J. O. Aidanpää, R. Perers, and M. Leijon, "Rotor dynamic analysis of an eccentric hydropower generator with damper winding for reactive load," *Journal of applied mechanics*, vol. 74, no. 6, pp. 1178–1186, 2007.
[37] S. Keller, M. T. Xuan, J. J. Simond, and A. Schwery, "Large low-speed hydro-generators - unbalanced magnetic pulls and additional damper losses in eccentricity conditions," *IET Electric Power Applications*, vol. 1, pp. 657–664, Sept 2007.
[38] M. Wallin, M. Ranlöf, and U. Lundin, "Reduction of unbalanced magnetic pull in synchronous machines due to parallel circuits," *IEEE Transactions on Magnetics*, vol. 47, pp. 4827–4833, Dec 2011.
[39] A. Burakov and A. Arkkio, "Comparison of the unbalanced magnetic pull mitigation by the parallel paths in the stator and rotor windings," *IEEE Transactions on Magnetics*, vol. 43, pp. 4083–4088, Dec 2007.
[40] A. Burakov and A. Arkkio, "Low-order parametric force model for eccentric-rotor electrical machine equipped with parallel stator windings and rotor cage," *IET Electric Power Applications*, vol. 1, pp. 532–542, July 2007.
[41] A. Laiho, A. Sinervo, J. Orivuori, K. Tammi, A. Arkkio, and K. Zenger, "Attenuation of harmonic rotor vibration in a cage rotor induction machine by a self-bearing force actuator," *IEEE Transactions on Magnetics*, vol. 45, pp. 5388–5398, Dec 2009.
[42] D. G. Dorrell, J. K. H. Shek, M. A. Mueller, and M. F. Hsieh, "Damper windings in induction machines for reduction of unbalanced magnetic pull and bearing wear," *IEEE Transactions on Industry Applications*, vol. 49, pp. 2206–2216, Sept 2013.
[43] R. El-Mahayni, K. Al-Qahtani, and A. H. Al-Gheeth, "Large synchronous motor failure investigation: Measurements, analysis, and lessons learned," *IEEE Transactions on Industry Applications*, vol. 52, pp. 5318–5326, Nov 2016.
[44] J. Nevelsteen and H. Aragon, "Starting of large motors-methods and economics," *IEEE Transactions on Industry Applications*, vol. 25,

pp. 1012–1018, Nov 1989.
[45] K. LeDoux, P. W. Visser, J. D. Hulin, and H. Nguyen, "Starting large synchronous motors in weak power systems," *IEEE Transactions on Industry Applications*, vol. 51, pp. 2676–2682, May 2015.
[46] A. T. de Almeida, F. J. T. E. Ferreira, and G. Baoming, "Beyond induction motors ;technology trends to move up efficiency," *IEEE Transactions on Industry Applications*, vol. 50, pp. 2103–2114, May 2014.
[47] C. Debruyne, M. Polikarpova, S. Derammelaere, P. Sergeant, J. Pyrhönen, J. J. M. Desmet, and L. Vandevelde, "Evaluation of the efficiency of line-start permanent-magnet machines as a function of the operating temperature," *IEEE Transactions on Industrial Electronics*, vol. 61, pp. 4443–4454, Aug 2014.
[48] M. A. Rahman, A. M. Osheiba, K. Kurihara, M. A. Jabbar, H. W. Ping, K. Wang, and H. M. Zubayer, "Advances on single-phase line-start high efficiency interior permanent magnet motors," *IEEE Transactions on Industrial Electronics*, vol. 59, pp. 1333–1345, March 2012.
[49] R. T. Ugale and B. N. Chaudhari, "Rotor configurations for improved starting and synchronous performance of line start permanent-magnet synchronous motor," *IEEE Transactions on Industrial Electronics*, vol. 64, pp. 138–148, Jan 2017.
[50] A. Castagnini, T. Känsäkangas, J. Kolehmainen, and P. S. Termini, "Analysis of the starting transient of a synchronous reluctance motor for direct-on-line applications," in *2015 IEEE International Electric Machines Drives Conference (IEMDC)*, pp. 121–126, May 2015.
[51] J. Tampio, T. Känsäkangas, S. Suuriniemi, J. Kolehmainen, L. Kettunen, and J. Ikäheimo, "Analysis of direct-on-line synchronous reluctance machine start-up using a magnetic field decomposition," *IEEE Transactions on Industry Applications*, vol. 53, pp. 1852–1859, May 2017.
[52] K. Ajiro, T. Inoue, and S. Satô, "Improvement of generator efficiency," *Fuji Electric Review*, vol. 28, no. 2, pp. 52–58, 1982.
[53] B. S. Herbage, "High efficiency fluid film thrust bearings for turbomachinery," in *Proceedings of the Sixth Turbomachinery Symposium*, pp. 33–38, 1977.
[54] Y. Adachi, S. Horie, and K. Yoshida, "30,000kva hydorogen-cooled vertical type sychronous condenser with magnetic bearing," *Fuji Denki Review*, vol. 2, no. 4, pp. 93–103, 1956.
[55] T. Nakata, "Magnetic thrust bearings," *Fuji Denki Review*, vol. 4, no. 2, pp. 33–40, 1958.
[56] A. Imanishi and M. Tomimura, "Main electric apparatus delivered to the hokuriku electric power co. wadagawa no.2 power station," *Fuji Denki Review*, vol. 5, no. 4, pp. 115–127, 1959.
[57] T. Nakata, R. Kuramochi, and S. Horie, "Generator-motor for hatanagi pumping-up power station, chubu electric power co., inc.," *Fuji Denki Review*, vol. 9, no. 1, pp. 1–12, 1963.
[58] A. Imanishi, T. Ueda, T. Nakada, and Y. Kawagoe, "Fuji hydraulic turbine and generator (i)," *Fuji Electric Review*, vol. 10, no. 5, pp. 164–174, 1964.
[59] S. Sato and H. Kadosaki, "The latest research for thrust bearing," *Fuji Electric Review*, vol. 28, no. 1, pp. 23–27, 1982.
[60] K. Yamaishi, "Applications and performance of magnetic bearing for water

turbine generator," in *Proceedings of MAG '97 Industrial conference and exhibition on magnetic bearings*, pp. 25–33, 1997.
[61] A. Imanishi, T. Ueda, T. Nakada, and Y. Kawagoe, "Fuji hydraulic turbine and generator (ii)," *Fuji Electric Review*, vol. 10, no. 6, pp. 198–206, 1964.
[62] T. Ueda, Y. Niikura, K. Ajiro, S. Sato, and A. Oshitani, "Site test of 500m 206mw pump-turbine and 220mva generator-motor," *Fuji Denki Review*, vol. 26, no. 3, pp. 72–81, 1980.
[63] T. Okuno, R. Ujiie, and Y. Yanagiya, "Results of field test of large generator and static converter starting system (for palmiet pumped storage power station)," *Fuji Electric Review*, vol. 36, no. 2, pp. 77–, 1990.
[64] Voith Siemens Hydro Power GmbH, "Modernization of europe's largest solution," in *HyPower 2*, pp. 38–41, 2002.
[65] S. Roberts and J. A. Brandon, "An investigation into the development of a condition monitoring/fault diagnostic system for large reversible francis type pump-turbines," in *Proceedings of the 14th International Conference on Condition Monitoring and Diagnostic Engineering Management*, pp. 135–142, Sept 2001.
[66] M. W. Garrett, "Calculation of fields, forces, and mutual inductances of current systems by elliptic integrals," *Journal of Applied Physics*, vol. 34, pp. 2567–2573, Sep 1963.
[67] Y. Iwasa, *Case Studies in Superconducting Magnets*. Springer US, 2nd ed., 2009.
[68] J. C. Maxwell, *A Treatise on Electricity and Magnetism, vol. 2*. Oxford University Press, 3rd ed., 1891.
[69] R. Ravaud, G. Lemarquand, S. Babic, V. Lemarquand, and C. Akyel, "Cylindrical magnets and coils: Fields, forces, and inductances," *IEEE Transactions on Magnetics*, vol. 46, pp. 3585–3590, Sept 2010.
[70] M. Hedlund, J. Abrahamsson, J. J. Pérez-Loya, J. Lundin, and H. Bernhoff, "Eddy currents in a passive magnetic axial thrust bearing for a flywheel energy storage system," *International Journal of Applied Electromagnetics and Mechanics*, vol. 54, pp. 389–404, July 2017.
[71] S. Sjökvist and S. Eriksson, "Experimental verification of a simulation model for partial demagnetization of permanent magnets," *IEEE Transactions on Magnetics*, vol. 50, pp. 1–5, Dec 2014.
[72] R. Perers, U. Lundin, and M. Leijon, "Saturation effects on unbalanced magnetic pull in a hydroelectric generator with an eccentric rotor," *IEEE Transactions on Magnetics*, vol. 43, pp. 3884–3890, Oct 2007.
[73] B. Marcusson and U. Lundin, "Axial magnetic fields, axial force, and losses in the stator core and clamping structure of a synchronous generator with axially displaced stator," *Electric Power Components and Systems*, vol. 45, no. 4, pp. 410–419, 2017.
[74] C. W.-R. Lee, W.-L. and W. Schumacher, "New approaches for axial magnetic bearings," in *Proceedings of ISMB7*, pp. 443–448, 2000.
[75] G. H. L.-R. Silber, S. and W. Amrhein, "Design aspects of bearingless torque motors," in *Proceedings of ISMB13*, pp. 1–12, 2012.
[76] A. W. B.-P. S. R. Silber, S. and N. Barletta, "Design aspects of bearingless slice motors," in *Proceedings of ISMB9*, 2004.

[77] N. Barletta and R. Schob, "Design of a bearingless blood pump," in *Proceedings of ISMST3*, pp. 265–274, 1995.
[78] C. R. Knospe and L. Zhu, "Performance limitations of non-laminated magnetic suspension systems," *IEEE Transactions on Control Systems Technology*, vol. 19, pp. 327–336, March 2011.
[79] L. Zhu, C. R. Knospe, and E. H. Maslen, "Analytic model for a nonlaminated cylindrical magnetic actuator including eddy currents," *IEEE Transactions on Magnetics*, vol. 41, pp. 1248–1258, April 2005.
[80] Y. Sun, Y. S. Ho, and L. Yu, "Dynamic stiffnesses of active magnetic thrust bearing including eddy-current effects," *IEEE Transactions on Magnetics*, vol. 45, pp. 139–149, Jan 2009.
[81] Z. W. Whitlow, R. L. Fittro, and C. R. Knospe, "Dynamic performance of segmented active magnetic thrust bearings," *IEEE Transactions on Magnetics*, vol. 52, pp. 1–11, Nov 2016.
[82] H. Wang, Y. Ye, Q. Wang, Y. Dai, Y. Yu, and P. Weng, "Analysis for ring arranged axial field halbach permanent magnets," *IEEE Transactions on Applied Superconductivity*, vol. 16, pp. 1562–1565, June 2006.
[83] M. Hongzhong, W. Qingyan, and J. Ping, "Study of the load reduction for hydro-generator bearing by hybrid magnetic levitation," *International Journal of Applied Electromagnetics and Mechanics*, vol. 43, no. 3, pp. 215–226, 2013.
[84] T. Lembke, "1-dof bearing arrangement with passive radial bearings and highly efficient integrated electrodynamic dampers, edd," in *Proceedings of ISMB13*, pp. 1–7, 2012.
[85] J. A. Walowit and O. Pinkus, "Analytical and experimental investigation of magnetic support systems. part 1: Analysis," *ASME Journal of Lubrication Technology*, vol. 104, pp. 418–428, July 1982.
[86] P. Albrecht, J. A. Walowit, and O. Pinkus, "Analytical and experimental investigation of magnetic support systems. part ll: Experimental investigation," *ASME Journal of Lubrication Technology*, vol. 104, pp. 429–437, July 1982.
[87] J. K. Nøland, F. Evestedt, J. J. Pérez-Loya, J. Abrahamsson, and U. Lundin, "Comparison of thyristor rectifier configurations for a six-phase rotating brushless outer pole pm exciter," *IEEE Transactions on Industrial Electronics*, vol. PP, no. 99, pp. 1–1, 2017.
[88] J. K. Nøland, F. Evestedt, J. J. Pérez-Loya, J. Abrahamsson, and U. Lundin, "Design and characterization of a rotating brushless outer pole pm exciter for a synchronous generator," *IEEE Transactions on Industry Applications*, vol. 53, pp. 2016–2027, May 2017.
[89] J. K. Nøland, *A new paradigm for large brushless hydrogenerators*. PhD thesis, Acta Universitatis Upsaliensis, 2017.
[90] T. Johansson, "Active rectification and control of magnetization currents in synchronous generators with rotating exciters: Implementation of the svpwm algorithm using mosfet technology," Master's thesis, Uppsala University, 2015.
[91] F. Evestedt, "Wireless control and measurement system for a hydropower generator with brushless exciter," Master's thesis, Uppsala University, 2015.
[92] M. Wallin, M. Ranlóf, and U. Lundin, "Design and construction of a synchronous generator test setup," in *The XIX International Conference on Electrical Machines - ICEM 2010*, pp. 1–5, Sept 2010.

[93] J. Weissbach, “Measuring forces on a hydropower generator using strain gages,” Master’s thesis, Uppsala University, 2015.
[94] Vattenfall AB and Centre for Business History, “The history and heritage of Vattenfall. The pioneer power stations..” Online, `http://history.vattenfall.com/`, Aug 2017.
[95] M. Cervantes, I. Jansson, A. Jourak, S. Glavatskih, and J.-O. Aidanpää, “Porjus u9 a full-scale hydropower research facility,” in *24th IAHR Symposium on Hydraulic Machinery and Systems*, Oct. 2008.
[96] K. Isaksson, S. Horneman, T. Hagelberg, and T. Ottosson, “Forskning i världsklass vid porjus vattenkraftcentrum,” *ABB Tidning*, no. 1,1999, pp. 28–34, 1999.
[97] M. Leijon, L. Gertmar, H. Frank, J. Martinsson, T. Karlsson, B. Johansson, K. Isaksson, and U. Wollström, “Breaking conventions in electrical power plants,” in *Cigre Session*, no. 11/37-03, 1998.
[98] M. Leijon, “Powerformer - a radically new rotating machine,” *ABB Review*, no. 2,1998, pp. 21–26, 1998.
[99] T. Karlsson, R. Olsson, M. Leijon, L. Gertmar, H. Frank, and P. Templin, “Non-conventional power plants,” in *12th CEPSI*, Nov. 1998.
[100] Wästfelt, L. Porjus power plant. 1914. Vattenfall AB and Centre for Business History. Online, `http://history.vattenfall.com/media-archive`, Aug 2017.
[101] Blomberg, H. Sverige, Porjus vattenkraftverk, Lule älv. 2007. Vattenfall AB. Online, `https://corporate.vattenfall.se/press-och-media/bildbank/`, Aug 2017.
[102] H. Henning, T. Hildinger, D. Ludwig, and M. Hagmeyer, “Fatigue assessment in hydro generator pole fixation,” in *Hydro Vision*, Oct 2015.
[103] EPRI, New England Power Co, New York Power Authority and Seattle City Light, “Advanced condition monitoring of hydrogenerators: knowledge base.” TR-114245, 1999.
[104] A. C. Meyer, E. Perrotti, L. C. Silva, and R. Ujiie, “Mancais de escora magnéticos,” in *XVI Seminário Nacional de Produção e Transmisşão de Energia Elétrica*, pp. 1–5, Oct 2001.
[105] G. Traxler-Samek, T. Lugand, and A. Schwery, “Additional losses in the damper winding of large hydrogenerators at open-circuit and load conditions,” *IEEE Transactions on Industrial Electronics*, vol. 57, pp. 154–160, Jan 2010.

Acta Universitatis Upsaliensis

Digital Comprehensive Summaries of Uppsala Dissertations from the Faculty of Science and Technology 1542

Editor: The Dean of the Faculty of Science and Technology

A doctoral dissertation from the Faculty of Science and Technology, Uppsala University, is usually a summary of a number of papers. A few copies of the complete dissertation are kept at major Swedish research libraries, while the summary alone is distributed internationally through the series Digital Comprehensive Summaries of Uppsala Dissertations from the Faculty of Science and Technology. (Prior to January, 2005, the series was published under the title "Comprehensive Summaries of Uppsala Dissertations from the Faculty of Science and Technology".)

Distribution: publications.uu.se
urn:nbn:se:uu:diva-328086

ACTA
UNIVERSITATIS
UPSALIENSIS
UPPSALA
2017